Chronostratigraphic framework and provenance of the Ossa-Morena Zone Carboniferous basins (SW Iberia)

M. Francisco Pereira[1*], Cristina Gama[1], Ícaro Dias da Silva I.[2], José B. Silva[3], Mandy Hofmann[4], Ulf Linnemann[4], Andreas Gärtner[4]

1- Instituto de Ciências da Terra, Departamento de Geociências, ECT, Universidade de Évora, Apt.94, 7002-554 Évora, Portugal

2- Instituto Dom Luiz, Faculdade de Ciências da Universidade de Lisboa, Campo Grande, 1749-016 Lisboa, Portugal

3- Instituto Dom Luiz, Departamento de Geologia, Faculdade de Ciências da Universidade de Lisboa, Campo Grande, 1749-016 Lisboa, Portugal

4- Senckenberg Naturhistorische Sammlungen Dresden, Museum für Mineralogie und Geologie, Germany

Correspondence to: M. Francisco Pereira (mpereira@uevora.pt)

Abstract. Carboniferous siliciclastic and silicic magmatic rocks from the Santa Susana-São Cristovão and Cabrela regions contain valuable information regarding the timing of synorogenic processes in SW Iberia. In this region of the Ossa-Morena Zone (OMZ), Late Carboniferous terrigenous strata (i.e. the Santa Susana Formation) unconformably overlie Early Carboniferous marine siliciclastic deposits alternating with volcanic rocks (i.e. the Toca da Moura volcano-sedimentary complex). Lying below this intra-Carboniferous unconformity, the Toca da Moura volcano-sedimentary complex is intruded and overlain by the Baleizão porphyry. Original SHRIMP and LA-ICP-MS U-Pb zircon are presented in this paper, providing chronostratigraphic and provenance constraints, since available geochronological information is scarce and only biostratigraphic ages are currently available for the Santa Susana-São Cristovão region. Our findings and the currently-available detrital zircon ages from Paleozoic terranes of SW Iberia (Pulo do Lobo Zone- PLZ, South-Portuguese Zone- SPZ, and OMZ), were jointly analyzed using the K-S test and MDS diagrams to investigate provenance. The marine deposition is constrained to the age interval of c. 335-331 Ma (Visean) by new U-Pb data for silicic tuffs from the Toca da Moura and Cabrela volcano-sedimentary complexes. The Baleizão porphyry, intrusive in the Toca da Moura volcano-sedimentary complex, yielded a crystallization age of c. 318 Ma (Bashkirian), providing the minimum age for the overlying intra-Carboniferous unconformity. A comparison of detrital zircon populations from siliciclastic rocks of the Cabrela and Toca de Moura volcano-sedimentary complexes of the OMZ suggests

that they derived from distinct sources more closely associated with the SPZ and PLZ than the OMZ. Above the intra-Carboniferous unconformity, the Santa Susana Formation is either the result of the recycling of distinct sources located in the Laurussian-side (SPZ and PLZ) and Gondwanan-side (OMZ) of the Rheic suture zone. The best estimate of the crystallization age of a granite cobble found in a conglomerate from the Santa Susana Formation yielded c. 303 Ma (Kasimovian-Gzhelian), representing the maximum depositional age for the terrestrial strata. The intra-Carboniferous unconformity seems to represent a stratigraphic gap of approximately 12-14 Ma, providing evidence of the rapid post-accretion/collision uplift of the Variscan orogenic belt in SW Iberia (i.e. the OMZ, PLZ and SPZ).

1. Introduction

The Variscan orogen that extends from central Europe to Iberia was reworked through discrete Carboniferous sedimentary cycles during the Laurussia-Gondwana convergence, giving rise to the formation of marine and terrestrial basins. In SW Iberia, stratigraphic correlation has been proposed for the Carboniferous synorogenic strata found in the three main tectonostratigraphic divisions of the Variscan Orogen: the Ossa-Morena (OMZ), Pulo do Lobo (PLZ) and South Portuguese (SPZ) zones (Quesada and Oliveira, 2019, and references therein).

The Carboniferous siliciclastic strata in the Santa Susana-São Cristovão and Cabrela regions (OMZ) includes fossils indicating Carboniferous to Kasimovian biostratigrapic ages (Teixeira, 1938-1940, 1941; Lemos de Sousa and Wagner, 1983; Wagner and Lemos de Sousa, 1983; Pereira et al., 2006; Machado et al., 2012; Lopes et al., 2014). In the Santa Susana-São Cristovão region, Late Carboniferous siliciclastic strata of the Santa Susana Formation unconformably overlie: i) the Baleizão volcanic-subvolcanic suite that was previously dated with whole-rock Rb-Sr isochrons (Priem et al., 1986), and ii) the early Carboniferous Toca da Moura volcano-sedimentary complex, which includes volcanic rocks that have never been dated. This intra-Carboniferous unconformity was generated as consequence of regional uplift and falling sea level, leading to a change in depositional environment from Early Carboniferous marine to Late Carboniferous terrestrial (Gonçalves and Carvalhosa, 1984; Oliveira et al., 1991; Machado et al., 2012). The provenance of the above-mentioned Carboniferous strata has been discussed based on petrographic, paleontological and detrital zircon geochronology evidence (Pereira et al., 2006; Machado et al., 2012; Lopes et al., 2014; Dinis et al., 2018).

In this paper, SHRIMP and LA-ICP-MS U-Pb analyses were performed on zircon grains from silicic volcanic, subvolcanic, and siliciclastic rocks sampled in the Santa Susana-São Cristovão and Cabrela regions (OMZ, SW Iberia). The aim of this geochronology study is to establish the chronostratigraphic framework of these Carboniferous strata and to discuss their provenance using a statistical approach (Kolmogorov-Smirnov test and Mutiscaling diagrams). Thus we pay

tribute to J.R. Martínez-Catalán, who devoted part of his career to investigating the Carboniferous synorogenic basins of NW Iberia.

2. Geological setting

In SW Iberia, the tectonic limit between the OMZ (Gondwanan-side) and the PLZ and SPZ (Laurussian-side) has been regarded as constituting the tectonically reworked suture zone of the Rheic Ocean (Andrade, 1983; Quesada et al., 1994; Simancas et al., 2005; Díaz-Apiroz et al., 2006; Ribeiro et al., 2007; Pereira et al., 2017a) (Fig. 1). This Paleozoic suture zone has been defined along the Beja-Acebuches ophiolitic complex (Fonseca et al., 1999, and references therein). The Beja-Acebuches ophiolitic complex is separated from the Beja Igneous Complex (Jesus et al., 2007, 2016) by a strike-slip fault. Metabasalts and metagabbros (i.e. the Mombeja unit of Andrade, 1983) from the Beja-Acebuches ophiolitic complex have been dated at c. 340-332 Ma (U-Pb zircon; Azor et al., 2008), while in the Beja Igneous Complex gabbro and granitic rocks are relatively older, yielding crystallization ages of c. 353-342 Ma (U-Pb zircon; Jesus et al., 2007; Pin et al., 2008). Trace element and isotopic signatures of Beja Igneous Complex plutonic rocks indicate crustal contamination of parental magmas deriving from a depleted asthenospheric mantle reservoir (Santos et al., 1990; Pin et al., 2008; Jesus et al., 2016). The plutonic rocks of the Beja Igneous Complex show well-defined intrusive contacts with previously deformed and metamorphosed sedimentary and igneous rocks of the OMZ basement (Rosas et al., 2008; Pin et al., 2008). The Beja Igneous Complex also includes the São Cristovão-Alcáçovas subvolcanic complex (Gonçalves and Carvalhosa, 1984), composed of silicic sub-volcanic and volcanic rocks (i.e. the Baleizão unit of Andrade, 1983), granophyres and porphyries dated at c. 319 Ma (whole-rock Rb-Sr isochrons; Priem et al., 1986), associated with diabases. Porphyry dykes are found cutting across the OMZ basement that is here formed by Cambrian igneous rocks with c. 527 Ma (Alcáçovas gneiss, Chichorro et al., 2008) deformed and metamorphosed in the Early Carboniferous at 340 ± 6 Ma (Pereira et al., 2009). The major and trace element geochemistry of the Baleizão porphyries indicates a calc-alkaline rhyolitic, rhyodacitic and andesitic composition typical of magmas produced at convergent plate boundaries (Santos et al., 1987; Caldeira et al., 2007; Ferreira et al., 2014). The Baleizão porphyries occur as dykes and sills (Andrade, 1927) (Figs. 3a, b), overlying (Gonçalves and Carvalhosa, 1984) the Early Carboniferous siliciclastic and volcanic rocks of the Toca da Moura volcano-sedimentary complex (Santos et al., 1987, and references therein) (Fig. 2).

The Toca da Moura volcano-sedimentary complex is mainly composed of pelites (i.e. "Xistinhos"; Teixeira, 1944; Fig. 3a) and greywackes, associated with andesite-to-rhyolite volcanic rocks (lava flow and tuffs; Figs. 3c, d, e), andesitic basalt, chert layers (Gonçalves and Carvalhosa, 1984), and a few olistoliths of basalt and limestone. Siliciclastic rocks contain well-preserved in-situ palynomorph assemblages of Tournaisian to Visean age and reworked

palynomorphs ranging in age from the Middle Cambrian to the Early Tournaisian (Pereira et al., 2006; Lopes et al., 2014). Based on geochemical information, this volcanism was interpreted by Santos et al. (1987) as deriving from calc-alkaline magma produced in a continental magmatic arc. A stratigraphic correlation was established between the Toca da Moura volcano-sedimentary complex and the Cabrela volcano-sedimentary complex (Pereira et al., 2006) which is located 15 km to the NW, in the Évora Massif (Pereira et al., 2007; 2012a) (Fig. 1b). The presence of variable-scale soft-sediment structures (i.e. slumps, intraclast conglomerates and olistoliths) in both complexes indicates gravity-induced instability during marine sedimentation. Detrital zircon ages of a siliciclastic rock from the Cabrela volcano-sedimentary complex interbedded with silicic tuffs (Fig. 3f) are mainly Middle-Late Devonian (82%) and Early Carboniferous (14%), also including a few older grains (sample OM-200 from Pereira et al., 2012a).

The Santa Susana Formation (i.e. Santa Susana basin, Domingos et al., 1983; Quesada et al., 1990, Oliveira et al. 1991) siliciclastic rocks that outcrop along a NNW-SSE-trending narrow discontinuous band which is 0.1-5 km wide and 12 km long unconformably overlie the Baleizão Porphyry and the Toca da Moura volcano-sedimentary complex (Fig. 2), forming the geological contact between these stratigraphic units often defined by faults (Gonçalves and Carvalhosa, 1984). The Santa Susana Formation is divided into two members (Machado et al., 2012, and references therein): i) the lower member is mainly composed of coarse-grained sandstone and conglomerate beds (Figs. 4a, b, c, d); these conglomerates include pebbles and cobbles of silicic porphyry, rhyolite, andesite, basalt, granite, felsic tuff, pelite, sandstone, greywacke, quartzite, phyllite, chert, and quartz (Figs. 4e, f); ii) the upper member represents a repetitive sequence of alternating beds of pelite and sandstone interbedded with coal seams, and few beds of conglomerate (Fig. 2). These terrestrial deposits were most probably deposited in an alluvial/fluvial-to-fluvial/lacustrine (floodplain lakes and/or abandoned channels with abundant vegetation) system (Machado et al., 2012, and references therein). The plant fossils identified in the siliciclastic rocks of the Santa Susana Formation indicate a Moscovian-Kasimovian biostratigraphic age (Wagner and Lemos de Sousa, 1983). Pelitic beds from the Upper member include palynomorph assemblages assigned with Kasimovian age (Machado et al., 2012). Palynomorphs ranging in age from the middle Cambrian to the early Moscovian were also found in siliciclastic rocks of the Santa Susana Formation sampled from a borehole at a depth of around 400 m (Lopes et al., 2014). Detrital zircon ages from upper member sandstones (Dinis et al., 2018) are mainly distributed over Devonian-Carboniferous (41-51%), Paleoproterozoic (23-30%) and Ediacaran-Cryogenian (16-23%) groups, and also a few Stenian-Tonian and Archean grains.

3. Rational and analytical methods

U-Pb geochronology of detrital zircon from siliciclastic rocks has been extensively used in stratigraphic correlation studies for estimating the maximum depositional age and investigating the provenance of sedimentary sequences (Fedo et al., 2001; Dickinson and Gehrels, 2009). The youngest detrital zircon grains found in siliciclastic rock commonly provide useful information about depositional age, especially in areas that experienced active volcanism during sediment accumulation (Geherls, 2014). The maximum depositional age obtained for siliciclastic rock is often not necessarily coincident with the biostratigraphic age as defined by key fossil assemblages (Pereira et al., 2019). Therefore, in order to overcome any doubt about the true age of deposition, it is desirable that volcanic rocks interstratified with fossiliferous siliciclastic rocks should be dated (Fedo et al., 2001; Bowring et al., 2006). Furthermore, the application of zircon U-Pb geochronology to volcano-sedimentary and sedimentary sequences that are separated by unconformities, by means of the comparative analysis of their age populations, may be useful for estimating time intervals and revealing changes in provenance. Volcanic rocks that lie beneath or overlie sedimentary sequences and unconformities can provide maximum and minimum ages, respectively. When detrital zircon geochronology is linked to the geochronology of crosscutting younger igneous rocks, then both a maximum and minimum age bracket for deposition can be determined (Fedo et al., 2001).

In this study, SHRIMP U-Pb analyses were performed for the first time on magmatic zircon from two tuffs from the Toca da Moura volcano-sedimentary complex (TM-1 and SCV-2; Figs. 3c, d), one tuff from the Cabrela volcano-sedimentary complex (CBR-12), one from the Baleizão silicic porphyry (SCV-30; Fig. 3b), and a cobble of granite (SCV-7; Fig. 4e) found in a conglomerate from the lower member of the Santa Susana Formation. Estimations of the crystallization age of samples SCV-2, TM-1 and CBR-12 (syndepositional volcanism), and sample SCV-30 (post-depositional) were used to validate the Tournaisian-Visean biostratigraphic age previously attributed to the Toca da Moura and Cabrela volcano-sedimentary complexes based on palynlogical assemblages (Pereira et al., 2006; Lopes et al., 2014). The presence of granite cobbles and pebbles in conglomerate layers from the lower Santa Susana Formation indicates denudation and recycling of a crystalline basement involving granite whose age is unknown. The dating of the granite cobble (sample SCV-7) is useful for discussing provenance and estimating the maximum depositional age of the Santa Susana conglomerate. In addition, LA-ICP-MS U-Pb analyses were performed on detrital zircon grains from two samples of sandstone from the upper and lower members of the Santa Susana Formation (samples SS-1 and SS-2, respectively; Fig. 5g, h), and a sample of pelite from the Toca da Moura volcano-sedimentary complex (sample TM-3; Fig. 5e). This new U-Pb data is useful for discussing provenance and determining the maximum depositional ages of the two sedimentary sequences separated by an intra-Carboniferous unconformity. Sample locations in the Santa Susana-São Cristovão region are indicated in Figure 2. Finally, detrital zircon grains

of siliciclastic rock from the Cabrela volcanic-sedimentary complex (sample CBR-11; Fig. 5f; equivalent to sample OM-200 of Pereira et al. 2012a) were analyzed to test for the existence of pre-Devonian ages. The new U-Pb results obtained in the present study are compared with previously-reported age spectra for pre-Kasimovian siliciclastic rocks from the OMZ, PLZ and SPZ siliciclastic sequences of SW Iberia, using statistical tools.

Zircon grains for U-Pb geochronology were selected using traditional techniques: density separation using a wilfley table (Universidad Complutense de Madrid, Spain) and also using granulometric separation using sieves with a mesh size of less than 500 microns, density (panning) separation procedures, and mineral identification using a binocular lens and preparation of epoxy resin mounts with zircon grains (Universidade de Évora, Portugal). U-Pb measurements were obtained at IBERSIMS (Universidad de Granada, Spain) using SHRIMP, and also at the Senckenberg Naturhistorische Sammlungen Dresden (Museum für Mineralogie und Geologie, Germany) using a LA-ICP-MS. U-Pb measurements using SHRIMP and LA-ICP-MS followed the procedures previously described by Dias da Silva et al. (2018) and Pereira et al. (2012a), respectively. U-Pb results are listed in Tables S1 and S2 (Supplementary Material). Concordia curves and weighted-average means were obtained using Isoplot 4 (Ludwig, 2003) (Figs. 6 and 7). Kernel density estimation (KDE) diagrams were produced with 90-110 % concordant $^{206}Pb/^{238}U$ ages for grains younger than 1.0 Ga, and $^{207}Pb/^{206}Pb$ ages for older grains (for further details, see Frei and Gerdes, 2009) using IsoplotR (Vermeesch, 2018) (Figs. 8a, b). Cathodoluminescence-imaging was performed at TU Bergakademie Freiberg (Germany) and at IBERSIMS.

The K-S test and the MDS technique were used in conjunction to compare populations of detrital zircon U-Pb ages obtained from the Carboniferous siliciclastic rocks of the Santa Susana-São Cristovão region using a method designed for a recent study of the provenance of Triassic sandstones (Gama et al., in press, and references therein). The K-S test is a non-parametric statistical tool that has been successfully used for the comparison of two populations of detrital zircon U-Pb ages by evaluating whether they are significantly different, i.e. indicating whether zircon age populations correlate with a similar source or not, regardless of whether they are of different sizes, while including at least 20 measurements (DeGraaff-Surpless et al., 2003). The probability of the observed maximum vertical difference between the cumulative probability curves (D-value) being unrelated to age differences between the two detrital zircon populations is given by a P-value corresponding to a confidence interval of 95% (Barbeau Jr. et al.; 2009; Guynn and Gehrels, 2010) (Fig. S1; supplementary material). High P-values and low D-values indicate that the observed difference between the two detrital zircon populations may be explained by the existence of common sources (Gama et al., 2020, and references therein). K-S analyses were carried out using an Excel spreadsheet published on the University of Arizona Geochronological Center website at

https://sites.google.com/a/laserchron.org/laserchron/. The MDS technique provides a means for the comparison of samples based on quantified pairwise comparisons of their detrital zircon ages, and is extremely useful for visualising the degree of similarity between samples in two dimensions, i.e. greater distances between samples represent a greater degree of dissimilarity between points on MDS diagrams (Vermeesch, 2013; Spencer and Kirkland, 2015; Wissink et al., 2018) (Fig. 9). MDS diagrams were produced using IsoplotR (Vermeesch, 2018).

4. U-Pb geochronology: Results

4.1. Volcanic silicic rocks of the Toca da Moura and Cabrela volcano-sedimentary complexes

Sample SCV-2 is a fine-grained banded rhyolitic tuff consisting of variable size and shape quartz and K-feldspar phenocrysts and lithoclasts (less than 1mm in diameter) dispersed in ash matrix (Fig. 5a). Zircon grains appear as stubby-to-elongated euhedral prisms (50-150 μm in diameter), mostly showing oscillatory concentric zoning growing on distinct cores or as simple crystals. There are some dark inclusions, unzoned patches and transgressive variably luminescence embayments. A total of 44 U-Th-Pb SHRIMP analyses of 44 grains yielded U content ranging from 262 to 628 ppm. A group of 23 grains with $^{206}Pb/^{238}U$ ages (discordance ≤ 5%) yielded a weighted mean $^{208}Pb/^{238}U$ age of 331 ± 4 Ma (MSWD = 1.2; Fig. 6a), which probably represents the crystallization age of tuff.

Sample TM-1 is a fine-grained banded rhyolitic tuff consisting quartz, K-feldspar and biotite phenocrysts, flattened dark-brown pumice (i.e. fiamme) and lithoclasts (less than 1mm in diameter) enclosed in ash matrix (Fig. 5b). The zircon population is characterized by stubby euhedral-to-sub-euhedral small (30-100 μm in diameter) grains. Magmatic grains are either simple with concentric zoning or composite showing variably luminescence cores with concentric zoning, unzoned, or banded zoned. These cores are surrounded by overgrowths with concentric zoning and are occasionally diffuse or unzoned. A total of 120 U-Th-Pb LA-ICP-MS analyses yielded U content ranging from 87 to 4136 ppm. 28 $^{206}Pb/^{238}U$ ages (90-110% of concordance) yield a weighted mean $^{208}Pb/^{238}U$ age of 341 ± 10 Ma with a very poor fit (MSWD = 6.9; Fig. 6b), as indicated by the scattering of ages along the Concordia curve. A coherent group of 21 grains with $^{206}Pb/^{238}U$ ages yielded a weighted mean $^{208}Pb/^{238}U$ age of 335 ± 6 Ma (MSWD = 1.5; Fig. 6b), providing the best age estimate for the volcanic rock (Fig. 6b). The youngest zircon grain (c. 302 Ma) probably experienced Pb loss. The six oldest zircon grains present Paleoproterozoic (c. 2 Ga), Neoproterozoic (c. 715 Ma) and Devonian (c. 395-378 Ma) ages, suggesting inheritance.

Sample CBR-12 is a fine-grained rhyolitic rock in which feldspar and quartz phenocrysts and lithic fragments occur embedded in altered very-fine grained matrix of quartz, sericite and chlorite, including devitrified shards. Zircon (40-150 μm in diameter) appears as stubby-to-

257 elongated euhedral prisms, mostly showing oscillatory concentric zoning, sometimes disturbed
258 by inclusions, as simple grains or as overgrowths. A few crystals show banded zoning or are
259 diffuse or unzoned. Thirty-two analyses were performed on this silicic volcanic rock yielding U
260 content ranging from 288 to 2587 ppm. Twenty-two analyses with discordance ≤ 5%, yielded a
261 weighted mean $^{208}Pb/^{238}Th$ age of 335 ± 2 Ma (MSWD = 1.2; Fig. 6c). The oldest two grains
262 yielding $^{206}Pb/^{238}U$ ages of c. 389 and 371 Ma are interpreted to represent xenocrysts.
263
264 **4.2. Baleizão porphyry**
265 Sample SCV-30 is a porphyritic rhyodacite-rhyolite consisting of quartz, plagioclase, K-
266 feldspar, biotite and amphibole phenocryst (less than 3mm in diameter) embedded in a fine-
267 grained silicic matrix (Fig. 5c). The zircon population contains grains (30-140 μm in diameter)
268 from subrounded subhedral to prismatic euhedral. Prisms are equant to moderately elongate
269 showing simple internal structure characterized by concentric and sector zoning to unzoned. A
270 concentric zoned or unzoned rim surrounds unzoned cores of few composite grains. A total of
271 37 U-Th-Pb SHRIMP analyses for sample SCV-30 yielded U content ranging from 74 to 4290
272 ppm. 25 analyses were obtained for zircon with discordance ≤ 5%, distributed along the
273 concordia curve from ca. 355 to 288 Ma, and yielded a weighted mean $^{208}Pb/^{238}Th$ age of 315 ±
274 6 Ma (mean square of weighted deviates, MSWD = 12; Fig. 7a). Some of the spread observed
275 could be due to the presence of inheritance. The oldest 10 grains yielding $^{206}Pb/^{238}U$ ages of c.
276 355-337 Ma probably represent xenocrysts derived from the Toca da Moura volcano-
277 sedimentary complex. Eleven grains in the age range ca. 334-311 Ma yielded a weighted mean
278 $^{208}Pb/^{238}U$ age of 318 ± 2 Ma (MSWD = 0.95; Fig. 7a), which is regarded as the best estimate
279 for the crystallization age of subvolcanic silicic rock.
280
281 **4.3. Cobble of granite found in a conglomerate from the Santa Susana Formation**
282 Sample SCV-7 is a cobble (20 cm in diameter) of pinkish medium-grained granite consisting of
283 quartz, alkali feldspar and biotite (Fig. 5d). Most zircons are stubby and elongated subeuhedral
284 to euhedral prisms (80 to 150 μm in diameter). Morphologically zircon grains are mostly simple
285 showing concentric zoning, sector zoning to unzoned, and few are composite with irregular and
286 unzoned small cores surrounded by a rim with concentric zoning. 40 U-Th-Pb SHRIMP
287 analyses were performed on sample SCV-7 with U content ranging from 348 to 3177 ppm. Of
288 this total of analyses 24 U-Pb ages with discordance ≤ 5%, scattered along the concordia curve
289 from ca. 349 to 294 Ma, yielded a weighted mean $^{206}Pb/^{238}U$ age of 327 ± 7 Ma (MSWD = 4;
290 Fig. 7b). A group of six zircon grains in the age range of c. 309-294 Ma yielded a weighted
291 mean $^{206}Pb/^{238}U$ age of 303 ± 6 Ma (MSWD = 0.98; Fig. 7b), which is taken as the probable
292 crystallization age of the granite. The remaining 19 zircon grains yielded $^{206}Pb/^{238}U$ ages of c.
293 349-326 Ma, suggesting inheritance.

294

295 **4.4. Siliciclastic rocks from the Toca da Moura and Cabrela volcano-sedimentary**
296 **complexes**

297 Sample TM-3 is a laminated poorly-sorted siltstone with quartz-rich silt layers, containing
298 feldspar and tourmaline grains, and lithoclasts (Fig. 5e), which are intercalated with darker
299 layers of clay. The zircon population is mostly characterized by stubby to elongated prismatic
300 small grains (less than 100 μm in diameter). It includes simple and composite zircons showing
301 concentric, sector and banded zoning. Of a total of 82 U-Th-Pb LA-ICP-MS analyses, with U
302 content ranging from 19 to 4630 ppm. 36 zircon grains yield 90-110% concordance. The
303 number grains of sample TM-1 is not conform to the minimum of 60-100 grains often used in
304 provenance studies (Vermeesch, 2004), and therefore percentages based on the proportions of
305 ages need to be interpreted with caution. The Paleozoic population of detrital zircon (36%)
306 includes Early Carboniferous (9%, c. 353, 349 and 340 Ma), Ordovician (14%, c. 476-456 Ma),
307 Cambrian (7%, c. 531-500 Ma) and Late Devonian (6%, c. 369 and 362 Ma) grains (Fig. 8a).
308 The Precambrian population (64%) is predominantly Neoproterozoic (36%; c. 983-587 Ma), but
309 also includes Paleoproterozoic (14%; c. 2-1.8 Ga), Mesoproterozoic (8%; c. 1.3-1 Ga) and
310 Archean (6%; c. 2.7-2.5 Ga) grains. The three youngest zircon grains (c. 353-340 Ma) yielded a
311 maximum depositional age of c. 348 Ma (Tournaisian), which is in accordance with the
312 sedimentary age inferred from biostratigraphic constraints (Late Tournaisian to Middle-Late
313 Viséan; Pereira et al., 2006; Lopes et al., 2014).
314 Sample CBR-11 is a fine-grained poorly-to-moderate sorted siltstone consisting predominantly
315 of quartz and few feldspar grains and lithoclasts enclosed in silt-clay-sized particles (Fig. 5g).
316 Most of zircon grains are small (less than 100 μm in diameter), euhedral to subeuhedral. They
317 are simple grains (short, stubby to equant prisms) with oscillatory concentric and banded
318 zoning, and only few are composite grains with rounded cores. Of a total of 20 U-Th-Pb LA-
319 ICP-MS analyses, with U content ranging from 54 to 1379 ppm, 10 grains yielded 90-110% of
320 concordance. Five grains are Paleozoic (Carboniferous: c. 359, 351 and 346 Ma; Cambrian: c.
321 514 and 511 Ma) and five are Precambrian (Paleoproterozoic: c. 2.4, 2.1 and 1.8 Ga;
322 Mesoproterozoic: 1 Ga; Neoproterozoic: c. 603 Ma). By combining our new data with those
323 from sample OM-200 (Pereira et al., 2012a) collected from the same quarry of sample CBR-11,
324 it was found that the detrital zircon population (CB, N = 54; Fig. 8a) is largely dominated by
325 Paleozoic grains (90%): Late-Middle Devonian (68%), Early Carboniferous (15%), Cambrian
326 (4%) and Early Devonian (2%) grains, being distinct from sample TM-3 described above (Fig.
327 8a). The number grains of sample CB (N=54), despite being larger than that of sample TM-1, is
328 not conform to the minimum of 60-100 grains, and therefore the proportions of ages obtained
329 also need to be interpreted with caution. The youngest zircon population (N = 5) ranging from c.
330 353 to 346 Ma), suggest a Tournaisian maximum depositional age which is slightly older than

the sedimentary age inferred from biostratigraphic constraints (Late Tournaisian to Middle-Late Viséan; Pereira et al., 2006).

4.5. Siliciclastic rocks from the Santa Susana Formation

Sample SS-2 represents medium-to-coarse grained poorly-sorted sandstone. It is mainly composed of lithoclasts (siltstone, mudstone, quartzite, phyllite, rhyolite, basalt) and quartz grains, but also includes muscovite and feldspar grains (Fig. 5g). The zircon population is mostly characterized by stubby to prismatic, subrounded to subangular, grains (120-300 μm in diameter). Morphologically were found simple and composite grains. Cathodoluminescence imaging shows that most zircon grains have concentric oscillatory zoning, irregular zoning and are banded or unzoned. A total of 153 U-Th-Pb LA-ICP-MS analyses were performed on detrital zircon grains. They show U content ranging from 15 to 6158 ppm. A population with 51 grains yielding U-Pb ages with 90-110% concordance (Fig. 8b) is dominated by Precambrian ages (64%): Neoproterozoic (37%; c. 801-551 Ma), Paleoproterozoic (25%; c. 2.4-1.6 Ga) and Neorchean (2%, c. 2.5 Ga). The Paleozoic grains (36%) are Carboniferous (20%; c. 359-303 Ma), Late Devonian (14%; c. 378-362 Ma), and Early Ordovician (2%; c. 447 Ma). The youngest two grains (303±4 Ma; Kasimovian-Gzhelian) are slightly younger than the sedimentary age inferred from biostratigraphic constraints (Middle Moscovian to Kasimovian; Lemos de Sousa and Wagner, 1983; Machado et al., 2012; Lopes et al., 2014).

Sample SS-1 represents a very-coarse grained sandstone consisting of rounded-to-subangular mono- and polycrystalline quartz, feldspar and muscovite grains, and a wide variety of lithoclasts (chert, phyllite, rhyolite, siltstone and sandstone; Fig. 5h) . Zircon grains are rounded to subangular, stubby and elongated prisms (less than 280 μm in diameter). The zircon population includes simple grains with oscillatory concentric, banded and sector zoning, and composite grains with cores with distinct internal morphologies surrounded by variable width rims. A total of 150 U-Th-Pb LA-ICP-MS analyses performed on detrital zircon grains yielded U content ranging from 24 to 9819 ppm. A group of 71 grains yielding U-Pb ages with 90-110% concordance are dominated by Paleozoic ages (82%), predominantly made up of Carboniferous (49%; c. 358-315 Ma) and Devonian (25%; c. 389-359 Ma), and a few Late Ordovician-Silurian (5%; c. 434, 429 and 425 Ma) and Cambrian (3%; c. 533 and 491 Ma) grains (Fig. 8b). The Precambrian grains (18%) are Neoproterozoic (10%; c. 702-542 Ma), Paleoproterozoic (4%; c. 2.1-1.6 Ga), Mesoproterozoic (3%, c. 1.4 and 1.6 Ga) and Neorchean (1%, c. 2.8 Ga). The youngest zircon population (N = 3; c. 319-315 Ma) suggest a Bashkirian maximum depositional age, which is slightly older than the sedimentary age inferred from biostratigraphic constraints (Middle Moscovian to Kasimovian; Lemos de Sousa and Wagner, 1983; Machado et al., 2012; Lopes et al., 2014).

5. K-S test and MDS analysis: results

We recognize that the representativeness of the detrital zircon grains of samples TM-1 and CB is not the most recommended for provenance analysis. However, we consider important to present a preliminary comparison of detrital zircon populations of Visean marine siliciclastic rocks from the Toca da Moura and Cabrela volcano-sedimentary complexes because it makes us suspect of variability in the sources.

The K-S test performed on the Santa Susana sandstones show that the detrital zircon populations of sample SS-2 (lower member) and SS upper member (i.e. includes samples StSz2 and StSz4 from Dinis et al., 2018) are 'not significantly different' (all ages- P-value = 0.169; pre-Carboniferous ages- P-value = 0.879) at the 5% confidence level (Fig. S1). A comparison of samples SS-1 and SS-2 reveals that they are "significantly different" (P-value ≤ 0.01). Unlike sample SS-2, the sample SS-1 detrital zircon population is "significantly different" (P-value < 0.01) from the SS upper population (Fig. S1), indicating that they derived from distinct sources. Besides this, sample SS-1 is much closer to that of the SS upper (D-value = 0.323), and more distant from sample SS-2 (D-value = 0.465) as regards the distance between cumulative probability curves (Fig. 8c).

In Figure 9a, the MDS diagram produced with all ages shows sample SS-1 adjacent to Cabrela and Mértola siliciclastic rocks, while sample SS-2 is near the Mira, Santa Iria and Represa detrital zircon populations. In the MDS diagram for pre-Carboniferous ages, sample SS-2 is juxtaposed with sample TM-3, and closest to the Mira, Phyllite-Quartzite and Tercenas formations (Fig. 9b) suggesting likely sources. Nevertheless, the probable contribution to SS-2 samples of sediment derived from the oldest siliciclastic rocks from the PLZ and SPZ (i.e. Pulo do Lobo, Gafo, Ribeira de Limas, Atalaia and Ronquillo formations), and OMZ sources cannot be excluded. Their detrital zircon populations are 'not enough significantly different' (all ages- P-value = 0.003), and 'not significantly different' (pre-Carboniferous ages- P-value = 0.113-0.165) at the 5% confidence level (Fig. S1). This similarity is also illustrated in the approximation between SS-2, P-G-R-A-R and OMZ populations in the MDS diagrams (Figs. 9a, b).

K-S test results for the comparison between samples SS-2 and TM-3 indicate that they present 'not significantly different' detrital zircon populations (all ages- P-value = 0.399; pre-Carboniferous ages- P-value = 0.0.411) at the 5% confidence level (Fig. S1). Furthermore, their cumulative probability curves are much closer (Fig. 8d): D-values are 0.195 (all ages) and 0.203 (pre-Carboniferous ages) (Fig. S1). The close relationship of the two detrital zircon populations suggests that the Toca da Moura volcano-sedimentary complex directly supplied sediment to the Santa Susana basin. However, the relationship described above does not extend to the entire Santa Susana basin since sample SS-1 presents a greater degree of similarity with the Cabrela

detrital zircon population as regards the proximity between cumulative probability curves (Fig. 8d) and MDS diagrams (Figs. 9a, b).

In addition, Cabrela siliciclastic rocks are 'significantly different' at the 5% confidence level from sample TM-3 (P-values < 0.01) as regards the significant distance between them on the MDS diagram (Figs. 9a, b), and the significant distance between cumulative curves (Fig. 8d), with a D-value interval of 0.712-0.731 (Fig. S1). The difference found in the detrital zircon populations suggests that Cabrela and Toca da Moura siliciclastic rocks probably derived from different sources.

As result of the K-S test and MDS analyisis, the Horta da Torre Formation is 'significantly different' (Fig. S1), and is clearly separate (Figs. 9a, b) from all the other detrital zircon populations, ruling out the possibility of it being a source for the Toca da Moura and Cabrela volcano-sedimentary complexes or Santa Susana Formation siliciclastic rocks.

6. Discussion

6.1. Chronostratigraphic framework

The geochronological data presented in the present study provide the basis for the first chronostratigraphic record for the Carboniferous basins of the Santa Susana-São Cristovão region (SW Iberia). Dating of silicic volcanic rocks interbedded in the Toca da Moura and Cabrela volcano-sedimentary complexes constrain an interval of felsic magmatism to occurring from c. 335 Ma to 331 Ma (Visean; Fig. 6), complementing currently-available biostratigraphic information for Toca da Moura and Cabrela siliciclastic rocks (Pereira et al., 2006; Lopes et al., 2014). U-Pb ages of the youngest detrital zircon grains from the siliciclastic rocks of the Toca da Moura and Cabrela volcano-sedimentary complexes (TM-3 and CB, respectively; Fig. 8a) provide maximum age constraints for these marine deposits. Their maximum depositional ages (c. 351-348 Ma; Tournaisian) are slightly older than currently-available biostratigraphic ages (Pereira et al., 2006; Lopes et al., 2014), but provide confirmation that both marine deposits are broadly contemporaneous.

Furthermore, the best estimate of the crystallization age of the Baleizão silicic intrusion provides a minimum age of 318 ± 2Ma (Bashkirian; Fig. 7a) for the intra-Carboniferous unconformity. Zircon extracted from a pebble of granite found in a Santa Susana conglomerate yielded a crystallization age of c. 303 Ma for plutonic rock (Fig. 7b). This age estimate overlaps the age interval of c. 305-303 Ma (i.e. the maximum depositional age range) obtained for the youngest population of detrital zircon grains from sandstone of the upper member (Dinis et al., 2018), complementing the currently-available biostratigraphic information for the Santa Susana Formation (Machado et al., 2012; Lopes et al., 2014). Given the findings described above, a stratigraphic interval of approximately 13-17 Ma can be established for the intra-Carboniferous unconformity, marking a change in depositional environment from marine to terrestrial in the

441 OMZ. Basin-drainage and infill patterns most probably changed due to rapid uplift of the
442 Variscan-Appalachian orogenic belt, active during the waning stages of Laurussia-Gondwana
443 collision (i.e. Late Carboniferous).
444
445 **6.2. Provenance and evolutionary model**
446 An initial important finding provides evidence that they derived from different sources. The
447 TM-3 population presents 64% Precambrian detrital zircon grains, while the CB population
448 contains only 10% (Fig. 8a). Toca da Moura siliciclastic rocks have a greater affinity with the
449 Phyllite-Quartzite, Tercenas, Santa Iria and Represa formations (Fig. 9), indicating that detrital
450 zircon populations were reproduced faithfully in SPZ and PLZ (Laurussian-type) sources. A
451 contribution from the oldest siliciclastic sequences of PLZ (Pulo do Lobo, Atalaia, Gafo and
452 Ribeira de Limas formations) and OMZ (Gondwanan-type) sources cannot be ruled out for
453 sample TM-3 (Fig. 9). The number of Late-Middle Devonian zircon grains in sample TM-3
454 (6%) is smaller than that of the CB population (68%) (Fig. 8a), suggesting that Cabrela
455 siliciclastic rocks were most likely derived largely from a Devonian source consistent with a
456 limited contribution from recycled ancient rocks (Pereira et al., 2012a). This indicates that the
457 origin of the Visean Toca da Moura and Cabrela basins is most likely more closely linked to
458 sources located in the SPZ and PLZ (Laurussian-type) than in the OMZ (Gondwanan-type). The
459 evidence in the Visean Toca da Moura basin for dissection of the inactive Devonian magmatic
460 arc and the erosion of its plutonic roots, together with the recycling of the PLZ and SPZ
461 Frasnian-Tournaisian siliciclastic sequences and OMZ basement rocks, differs from the
462 evidence in the Cabrela basin. The significance of the involvement of distinct sources is that
463 part of the region located on the boundary between the OMZ- PLZ and the SPZ (SW Iberia) was
464 subjected to uplift while the remaining part underwent flexural subsidence. A similar tectonic
465 setting has been put forward as an explanation for differences in stratigraphy found in the
466 Pedroches syn-orogenic basin located along the OMZ-Central Iberian Zone boundary
467 (Armendáriz et al., 2008, and references therein) (Fig. 1).
468 Over the past four decades, different models have emerged to explain the geodynamic evolution
469 of SW Iberia, with the subduction polarity being widely discussed (Quesada et al., 1994; Castro
470 et al., 1996; Ribeiro et al., 2007; Pin et al., 2008; Simancas et al., 2009; Braid et al., 2011;
471 Pérez-Cáceres et al. 2015a; Díez Fernández et al., 2016; Pereira et al., 2017a). Although in
472 many paleogeographic reconstructions for the Devonian, Iberia is flanked by the Rheic and
473 Paleotethys oceans (Stampfli et al., 2002, 2013; Cocks and Torsvik, 2006; Stampfli and Kozur,
474 2006; Torsvik et al., 2012; Arenas et al., 2014; von Raumer et al., 2016), solely the subduction
475 of Rheic Ocean is considered in the present geodynamic models for Iberia. This geodynamic
476 model of a single ocean has been the trigger of numerous discussions about whether the active
477 magmatic arc was located in Laurussia or Gondwana margins. Our challenging recent proposal

478 considers that SW Iberia geodynamic evolution could have been linked to the closure of these
479 two oceanic basins (Pereira et al., 2020). The main assumption that we must assume is that SPZ
480 and PLZ (Laurussian-side) and OMZ (Gondwana-side) have experienced different and
481 independent geodynamic evolutions before they were juxtaposed by the Variscan sinistral
482 orogen-parallel motion (Pérez-Cáceres et al., 2015b). As illustrated in Figure 10a, the
483 subduction of the Rheic Ocean floor beneath the Laurussian margin during the Late Devonian
484 (Pérez-Cáceres et al., 2015a; Pereira et al., 2017a, and references therein) caused the onset of
485 the Rheic magmatic arc in the Meguma terrane and related synorogenic basins. A slab rollback
486 mechanism similar to the one that caused the opening of the Okinawa trough behind the
487 Ryukyu-type subduction in the Pacific Ocean (Yamaji, 2003; Boutelier and Cruden, 2013)
488 could explain the lithosphere extension in the Laurussian-side and the Late Devonian
489 siliciclastic sedimentation in SPZ and PLZ (Pereira et al., 2017a). The Laurussian active margin
490 was progressively accreted to the Gondwana passive margin facing the Rheic Ocean during the
491 Late Devonian (Fig. 10a). A nappe stack was gradually emplaced in the Gondwana margin as a
492 consequence of ongoing continental collision (Pérez-Cáceres et al., 2015a; Díez Fernández and
493 Arenas, 2015, and references therein; Díez Fernández et al., 2016) and orogenic gravitational
494 collapse (Dias da Silva et al., 2020). Following the closure of the Rheic, Tournaisian, magmatic
495 episodes were associated with lithospheric extension in the Laurussian (Pyrite belt volcano-
496 sedimentary complex and Gil Márquez pluton) and Gondwanan (Beja igneous complex)
497 margins. A mechanism of steepening and break-off of the Rheic Ocean slab beneath the
498 Laurussian margin, as the modern analog of Eastern Anatolia Alpine-Hymalaya collisional
499 mountain belt (Sengor et al., 2003; Keskin, 2007), possibly was the main the reason for the
500 Early carboniferous magma generation in the SPZ (Pin et al. 2008), simultaneously the Meguma
501 terrane experienced rapid uplift and terrestrial sedimentation (Fig. 10b1). At the same time, in
502 the Gondwanan-side, the upwelling of the asthenosphere could have triggered partial melting of
503 crustal materials, and lithosphere extension (Pereira et al., 2009; 2012b), creating the right
504 conditions for the onset of gneiss domes in the OMZ (Dias da Silva et al., 2018). The
505 emplacement of voluminous subduction-related magmas (Santos et al., 1990; Castro et al.,
506 1996; Jesus et al., 2007; Pin et al., 2008; Lima et al., 2012; Pereira et al., 2007, 2015a; Moita et
507 al., 2009, 2015), including some with boninitic (Castro et al., 1999) and adakitic (Lima et al.,
508 2013) affinities, was coeval with flexural subsidence, marine sedimentation and volcanism
509 (Toca da Moura, Cabrela, Los Pedroches basins) (Fig. 10b2). The Early Carboniferous thermal
510 anomaly recorded in the OMZ has been interpreted to result from the emplacement in the
511 middle crust of a large volume of mantle plume-related magmas (Simancas et al., 2006). Other
512 studies have suggested that voluminous Early Carboniferous magmatism could have resulted
513 from the subduction of an oceanic ridge, creating a slab window beneath the OMZ (Castro et al.,
514 1996, 1999; Diaz-Azpiroz et al., 2006). This model uses the Chile ridge that plunges beneath

South America Plate in Patagonia (Breitsprecher and Thorkelson, 2009) as modern analog. Our model assumes the subduction of a ridge of the Paleotethys Ocean lithosphere beneath the Gondwana margin (Fig. 10b2), instead of the Rheic Ocean lithosphere, as a hypothesis to be further explored since the magmatic activity has extended to the Serpukhovian and Bashkirian in the OMZ (Pavia pluton, Valencia del Ventoso plutonic complex and Baleizão porphyry). Simultaneously with the putative subduction of the Paleotethys Ocean ridge, other regions of the Appalachian-Variscan orogenic belt, mostly in the Laurussian-side (Fig. 10b1), have experienced an oblique collision, rapid uplift and terrestrial sedimentation (Pereira et al., 2020). A second significant finding is that detrital zircon populations from the Santa Susana Formation (samples SS-1 and SS-2) also show significant differences (Figs. 8 and 9). Basal conglomerate (sample SS-2) presents a greater percentage of Precambrian grains (64%) than uppermost sandstone (SS-1 sample; 28%), and presents a great degree of affinity with the detrital zircon population of sample TM-3. Sample SS-2 presents a great degree of similarity with the detrital zircon populations of overlying SS upper-member sandstones (samples StSz-2 and StSz-4; Dinis et al., 2018) sampled as part of the same stratigraphic profile. SS-2 and SS upper-age populations show a great degree of affinity (Fig. 9), suggesting that detrital zircon grains were mainly derived from the erosion of the Toca da Moura volcano-sedimentary complex, the Santa Iria and Represa formations (PLZ) and the Mira Formation (SPZ). However, regarding the detrital zircon grains with pre-Carboniferous ages, additional contributions from other PLZ (Pulo do Lobo, Atalaia, Gafo and Ribeira de Limas formations), SPZ (Brejeira, Phyllite-Quartzite, Tercenas and Ronquillo formations) and OMZ sources cannot be ruled out (Figs. 9a, c). The zircon age population of sample SS-1, which is distinct from the SS-2 population, presents a great degree of affinity with the CB population, suggesting lateral changes in sources during deposition of Santa Susana uppermost sandstones. The great degree of affinity of the SS-1, Cabrela volcano-sedimentary complex, with Mértola Formation detrital zircon populations suggests a close association between the two and a common source. Cabrela and Mértola siliciclastic rocks may be regarded as the main source for sample SS-1 and an intermediate sediment repository as they are derived from the erosion of a Devonian source partially represented by the Cercal porphyries from the SPZ. As result of rapid uplift, the progressive erosion of the Devonian magmatic arc (including its plutonic roots), and that of PLZ, SPZ and OMZ rocks, is evidenced in the Santa Susana Formation. The volumetrically significant contribution of Carboniferous sources to the Santa Susana basin fill confirms derivation from the erosion of: i) Pyrite Belt volcanic rocks, and Phyllite-Quartzite, Tercenas, Mértola, Mira and Brejeira siliciclastic rocks (SPZ); ii) the Santa Iria and Represas formations (PLZ); iii) Gil Marquez granitic rocks and other plutons of the Sierra del Norte Batholith (SPZ and PLZ); iv) the Beja igneous complex, which includes the Baleizão porphyries (OMZ), and Évora and Pavia plutonic and high-grade metamorphic rocks (OMZ); and v) the Cabrela and Toca da Moura

volcanic-sedimentary complexes (OMZ) and Mértola turbidites (SPZ). From Late Carboniferous to Early Permian, large-scale strike-slip motions have juxtaposed OMZ to PLZ and SPZ (García-Navarro and Fernández, 2004; Pérez-Cáceres et al., 2015b), simultaneously with the rapid uplift of Variscan orogenic belt (Fig. 10c). In Kasimovian-Ghzelian, sedimentation probably occurred through the opening of the pull-apart terrestrial basin (Santa Susana basin) related to the movement of major strike-slip faults (i.e. Porto-Tomar fault zone, Pereira et al., 2010; Machado et al., 2012; Gútiérrez-Alonso et al., 2015) during the progressive uplift and buckling of the linear Appalachian-Variscan orogenic belt (i.e. OMZ, PLZ and SPZ; Fig. 10c), related to a change in the regional stress-field that produced the Greater Cantabrian Orocline (Pastor-Galan et al., 2015). U-Pb dating of magmatic zircon extracted from a pebble of granite (c. 303 Ma; Fig. 7b) found in a conglomerate of the Santa Susana Formation lower member suggests provenance from the direct erosion of Permo-Carboniferous plutons (i.e. original primary source), such as Santa Eulália-Monforte granitic and gabbro-dioritic rocks (OMZ). This c. 303-297 Ma calc-alkaline plutonic suite is coeval with the Nisa-Albuquerque and Los Pedroches batholiths, located on the OMZ-Central Iberian Zone boundary (Fig. 1), probably representing magmatism related to the eastward-migration of the Paleotethyan arc (Permo-Carboniferous Pyrennes plutonic and volcanic rocks; Pereira et al., 2014; Pereira et al., 2015b, 2017b). The Permo-Carboniferous OMZ plutons were emplaced at shallow crustal levels consistent with the low assimilation of country rocks and the sharp contacts, and therefore, they may have experienced denudation shortly after its crystallization without being required unrealistic uplift rates.

7. Conclusions

The main conclusions of this study are the following:

1. Visean marine deposition in the Santa Susana-São Cristovão and Cabrela regions is constrained to the age interval of c. 335-331 Ma by the new U-Pb data for volcanic rocks intercalated within siliciclastic rocks of the Toca da Moura and Cabrela volcano-sedimentary complexes.

2. U-Pb dating of the Baleizão porphyry provides a minimum age of 318 ± 2Ma (Bashkirian) for the overlying intra-Carboniferous unconformity.

3. Visean siliciclastic rocks from the Cabrela and Toca de Moura volcano-sedimentary complexes are derived from distinct sources, which probably include a Devonian continental magmatic arc, and are likely to be more closely associated with the Laurussian-type sources (SPZ and PLZ) than the Gondwanan-type sources (OMZ).

4. Terrestrial siliciclastic rocks from the Santa Susana Formation are probably the result of the recycling of distinct sources associated with the SPZ, PLZ and OMZ.

5. The best estimate of crystallization of a granite pebble found in Santa Susana Formation conglomerate suggest a maximum depositional age of c. 303 Ma (Kasimovian-Gzhelian); together with the youngest U-Pb ages (< c. 318 Ma) of detrital zircon grains, these findings provide evidence of the denudation of primary crystalline sources during the rapid post-accretion/collision uplift of the Variscan orogenic belt in SW Iberia (i.e. Gondwanan- and Laurussian-type sources).

6. The intra-Carboniferous unconformity that separates the Toca da Moura volcano-complex and the Baleizão porphyry from the Santa Susana Formation indicates a notable time interval of approximately 13-17 Ma.

Acknowledgements

This work is a contribution to projects CGL2016-76438-P and PGC2018-096534-B-I00 (Spain), the ICT's Research Group 6- Lithosphere Dynamics (ICT-UID/GEO/04683/2019) and, IDL's Research Group 3- Solid Earth dynamics, hazards, and resources (Portuguese FCT). Í. Dias da Silva acknowledges financial support by SYNTHESIS3-ACCESS (DE-TAF-5798), FCT postdoctoral grant SFRH/BPD/99550/2014 and FCT-project UID/GEO/50019/2019-IDL. This is IBERSIMS publication number xx.

References

Andrade, A.S.: Contribuition à l'Analyse de la Suture Hercynienne de Beja (Portugal), Perspectives Métallogéniques. Unpublishe PhD thesis INPL, 137 p, 1983.

Andrade, C.F.: Alguns elementos para o estudo dos depósitos de carvão do Moinho da Ordem. Comunicações dos Serviços Geológicos de Portugal, tomo XVI, 3-28, 1927.

Arenas, R., Díez Fernández, R., Sánchez Martínez, S., Gerdes, A., Fernández-Suárez, J. and Albert, R.: Two-stage collision: exploring the birth of Pangea in the Variscan terranes. Gondwana Research 25, 756-763, 2014.

Armendáriz, M., López-Guijarro, R., Quesada, C., Pin, C. and Bellido, F.: Genesis and evolution of a syn-orogenic basin in transpression: Insights from petrography, geochemistry and Sm-Nd systematics in the Variscan Pedroches basin (Mississippian, SW Iberia). Tectonophysics 461: 395-413, 2008.

Azor, A., Rubatto, D., Simancas, J.F., González Lodeiro, F., Martínez Poyatos, D., Martín Parra, L.M. and Matas, J.: Rheic Ocean ophiolitic remnants in southern Iberia questioned by SHRIMP U-Pb zircon ages on the Beja-Acebuches amphibolites. Tectonics 27, TC5006, doi:10.1029/2008TC002306, 2008.

Barbeau, D.L., Davis , J.T., Murray, K.E., Valencia, V., Gehrels, G.E., Zahid, K.M. and Gombosi, D.J.: Detrital-zircon geochronology of the metasedimentary rocks of north-western Graham Land. Antarctic Science 22, 65-78, 2009.

Boutelier, D. and Cruden, A.: Slab rollback rate and trench curvature controlled by arc deformation. Geology v. 41; no. 8, 911-914, 2013.

Bowring, S.A., Schoene, B., Crowley, J.L., Ramezani, J. and Condon, D.J.: High-precision U-Pb zircon geochronology and the stratigraphic record: Progress and promise. In: Olszewski, T. (Ed.), Geochronology: Emerging Opportunities, Paleontological Society Short Course, October 21, Philadelphia, PA., Paleontological Society Papers, Volume 11, 23-43, 2006.

Braid, J.A., Murphy, J.B., Quesada, C. and Mortensen, J.: Tectonic escape of a crustal fragment during the closure of the Rheic Ocean: U–Pb detrital zircon data from the late Palaeozoic Pulo de Lobo and South Portuguese Zones, Southern Iberia, Journal of the Geological Society of London 168, 383–392, 2011.

Breitsprecher, K. and Thorkelson, D.J.: Neogene kinematic history of Nazca-Antarctic-Phoenix slab windows beneath Patagonia and the Antarctic Peninsula. Tectonophysics 464, 10-20, 2009.

Caldeira, R., Ribeiro, M.L. and Moreira, M.E. Geoquímica das sequências máficas e félsicas entre Alvito, Torrão e Alcáçovas (SW da ZOM). Comunicações Geológicas, 94, 5-28, 2007.

Cambeses, A., Scarrow, J.H., Montero, P., Molina, J.F. and Moreno, J.A. SHRIMP U-Pb zircon dating of the Valencia del Ventoso plutonic complex, Ossa-Morena Zone, SW Iberia: Early Carboniferous intra-orogenic extension-related 'calc-alkaline' magmatism. Gondwana Research 28, 735-756, 2015.

Castro, A., Fernández, C., de la Rosa, J.D., Moreno-Ventas, I., El Hmidi, H., El Biad, M., Bergamin, J.F. and Sánchez, N.: Triple-junction migration during Paleozoic Plate convergence: The Aracena metamorphic belt, Hercynian massif, Spain, Geologische Rundschau., 85, 108-185, 1996.

Castro, A., Fernández, C. El-Hmidi, H., El-Bia, M. Díaz Azpiroz, M., de la Rosa, J.D. and Stuart, F.: Age constraints to the relationships between magmatism, metamorphism and tectonism in the Aracena metamorphic belt, southern Spain, International Journal of Earth Sciences, 88, 26-37, 1999.

Chichorro, M., Pereira, M. F., Díaz-Azpiroz, M., Williams, I.S., Fernández, C., Pin, Ch., and Silva, J.B.: Cambrian ensialic rift-related magmatism in the Ossa-Morena Zone (Évora-Aracena metamorphic belt, SW Iberian Massif): Sm-Nd isotopes and SHRIMP zircon U-Th-Pb geochronology. Tectonophysics, 461, 91-113, 2008.

Cocks, L.R.M. and Torsvik, T.H.: European geography in a global context from the Vendian to the end of the Palaeozoic. In: Gee, D.G., Stephenson, R.A. (eds). European Lithosphere Dynamics. Geological Society, London, Memoirs, 32, 83-95, 2006.

DeGraaff-Surpless, K., Mahoney, J.B., Wooden, J.L. and McWilliams, M.O.: Lithofacies control in detrital zircon provenance studies: insights from the Cretaceous Methow Basin, Southern Canadian Cordillera. Geological Society of America Bulletin, 115(8), 899-915, 2003.

Dias da Silva, Í., González Clavijo, E. and Díez-Montes, A.: The collapse of the Variscan belt: a Variscan lateral extrusion thin-skinned structure in NW Iberia. International Geology Review, https://doi.org/10.1080/00206814.2020.1719544, 2020.

Dias da Silva, Í., Pereira, M.F., Silva, J.B., and Gama, C.: Time-space distribution of silicic plutonism in a gneiss dome of the Iberian Variscan Belt: The Évora Massif (Ossa-Morena Zone, Portugal). Tectonophysics 747-748, 298-317, 2018.

Díaz Azpiroz, M., Fernandez, C., Castro, A. and El-Biad, M.: Tectonometamorphic evolution of the Aracena metamorphic belt (SW Spain) resulting from ridge-trench interaction during Variscan plate convergence. Tectonics 25, http://dx.doi.org/ 10.1029/2004TC001742, 2006.

Dickinson, W.R. and Gehrels, G.E.: Use of U-Pb ages of detrital zircons to infer maximum depositional ages of strata: a test against a Colorado Plateau Mesozoic database. Earth and Planetary Science Letter 288, 115-125, 2009.

Díez Fernández, R., Arenas, R., Pereira, M.F., Sánchez Martínez, S., Albert, R., Martín Parra, L.M., Rubio Pascual, F.J. and Matas, J.: Tectonic evolution of Variscan Iberia: Gondwana-Laurussia collision revisited. Earth-Science Reviews 162, 269–292, 2016

Díez Fernández, R. and Arenas, R.: The Late Devonian Variscan suture of the Iberian Massif: a correlation of high-pressure belts in NW and SW Iberia. Tectonophysics 654, 96-100, 2015.

Dinis, P.A., Fernandes, P., Jorge, R.C.G.S., Rodrigues, B., Chew, D.M. and Tassinari, C.G.: The transition from Pangea amalgamation to fragmentation: constraints from detrital zircon geochronology on West Iberia paleogeography and sediment sources. Sedimentary Geology 375, 172-187, 2018.

Domingos, L.C.G., Freire, J.L.S., Silva, F. G., Gonçalves, F., Pereira, E. and Ribeiro, A.: The Structure of the Intramontane Upper Carboniferous Basins in Portugal. In: M. J. Lemos de Sousa, J.T. Oliveira (eds.), The Carboniferous of Portugal. Memorias, Nova Série 29, Serviços Geológicos de Portugal, Lisboa: 187-194, 1983.

Fedo, C.M., Sircombe, K.N. and Rainbird, R.H.: Detrital zircon analysis of the sedimentary record. In: Zircon (eds. M. Hanchar & P.W.O. Hoskin) Reviews in Mineralogy and Geochemistry, 53, 277-303. Mineral Society of America,Washington, DC, 2003.

Ferreira, P., Caldeira, R. and Calvo, R.: Geoquímica das rochas ígneas aflorantes na região de S. Matias, Cuba (Alentejo). Comunicações Geológicas (2014) 101, Especial I, 93-97, 2014.

Fonseca, P., Munhá, J., Pedro, J., Rosas, F., Moita, P., Araújo, A. and Leal, N.:Variscan ophiolites and high-pressure metamorphism in southern Iberia. Ofioliti 24, 259-268, 1999.

Frei, D. and Gerdes, A.:Precise and accurate in-situ U–Pb dating of zircon with high sample throughput by automated LA-SF-ICP-MS. Chemical Geology 261(3-4): 261-27, 2009.

Gama, C., Pereira, M.F., Crowley, Q.G., Dias da Silva, Í. and Silva, J.B.: Detrital zircon provenance of Triassic sandstone of the Algarve Basin (SW Iberia): Evidence of Gondwanan- and Laurussian-type sources of sediment. Geological Magazine, https://doi.org/10.1017/S0016756820000370, 2020.

García-Navarro, E, and Fernández, C.: Final stages of the Variscan Orogeny at the southern Iberian massif: Lateral extrusion and rotation of continental blocks. Tectonics 23, TC6001, DOI:10.1029/2004TC001646, 2004.

Gehrels, G.E.: Detrital zircon U-Pb geochronology applied to tectonics. Annual Review of Earth and Planetary Sciences 42: 127-149, 2014.

Gonçalves, F. and Carvalhosa, A.:Subsídios para o conhecimento geológico do Carbónico de Santa Susana Vol. D' Hommage au géologue G. Zbyszewski. Recherche de Civilisations, Paris, pp. 109-130, 1984.

Gutiérrez-Alonso, G., Collins, A.S., Fernández-Suárez, J., Pastor-Galán, D., González-Clavijo, E., Jourdan, F., Weil, A.B., and Johnston, S.T.: Dating of lithospheric buckling: $^{40}Ar/^{39}Ar$ ages of syn-orocline strike–slip shear zones in northwestern Iberia: Tectonophysics, 643, 44-54, 2015.

Guynn, J. and Gehrels, G.: Comparison of Detrital Zircon Age Distributions Using the K-S Test. Arizona LaserChron Center. Available at: https://laserchron.org/, 2010

Jesus, A., Munhá, J., Mateus, A., Tassinari, C. and Nutman, A.:The Beja layered gabbroic sequence (Ossa–Morena Zone, Southern Portugal): geochronology and geodynamic implications. Geodinamica Acta 20, 139-157, 2007.

Jesus, A.P., Mateus, A., Munhá, J.M., Tassinari, C.G., Bento dos Santos, T.M. and Benoit, M.: Evidence for underplating in the genesis of the Variscan synorogenic Beja Layered Gabbroic Sequence (Portugal) and related mesocratic rocks. Tectonophysics 683: 148-171, 2016.

Keskin, M.: Eastern Anatolia: A hotspot in a collision zone without a mantle plume. In: Foulger, G.R., Jurdy, D.M. (eds), Plates, plumes, and planetary processes: Geological Society of America Special Paper 430, 693-722, 2007.

Lemos de Sousa, M.J. and Wagner, R.H.: General description of the terrestrial Carboniferous basins in Portugal and history of investigations. In: Lemos de Sousa M.J. and Oliveira, J.T., (eds) The Carboniferous of Portugal. Memórias dos Serviços Geológicos de Portugal 29:117-126, 1983.

Lima, S.M., Corfu, F., Neiva, A.M.R. and Ramos, M.F.: Dissecting complex magmatic processes: an in-depth U-Pb study of the Pavia Pluton, Ossa-Morena Zone, Portugal. Journal of Petrology 53, 1887-1911, 2012.

Lima, S.M., Neiva, A.M.R. and Ramos, J.M.F.: Adakitic-like magmatism in western Ossa–Morena Zone (Portugal): Geochemical and isotopic constraints of the Pavia pluton. Lithos 160-161, 98-116, 2013.

Linnemann, U., Pereira, M.F., Jeffries, T., Drost, K. and Gerdes, A.: Cadomian orogeny and the opening of the Rheic Ocean: new insights in the diachrony of geo-tectonic processes constrained by LA-ICP-MS U–Pb zircon dating (Ossa-Morena and Saxo-Thuringian Zones, Iberian and Bohemian Massifs). Tectonophysics 461, 21-43, 2008.

Lopes, G., Pereira, Z., Fernandes, P., Wicander, R., Matos, J.X., Rosa, D. and Oliveira, J.T.: The significance of reworked palynomorphs (middle Cambrian to Tournaisian) in the Visean Toca daMoura Complex (South Portugal). Implications for the geodynamic evolution of Ossa Morena Zone. Review of Palaeobotany and Palynology 200, 1-23, 2014.

Ludwig, K.R.: Isoplot/Ex Version 3.0: a Geochronological Toolkit for Microsoft Excel, 2003.

Machado, G., Dias da Silva, I. and Almeida, P.: Palynology, stratigraphy and geometry of the Pennsylvanian continental Santa Susana Basin (SW Portugal). Journal of Iberian Geology 38, 429-448, 2012.

Moita, P., Santos, J.F. and Pereira, M.F.: Layered granitoids: interaction between continental crust recycling processes and mantle-derived magmatism. Examples from the Évora Massif (Ossa-Morena Zone, southwest Iberia, Portugal). Lithos 111, (3-4): 125-141, 2009.

783 Moita, P., Santos, J.F., Pereira, M.F., Costa, M.M. and Corfu, F.: The quartz-dioritic Hospitais intrusion
784 (SW Iberian Massif) and its mafic microgranular enclaves -evidence for mineral clustering. Lithos 224-
785 225, 78-100, 2015.
786
787 Oliveira, J.T., Oliveira, V. and Piçarra, J.: Traços gerais da evolução tectono-estratigráfica da Zona de
788 Ossa Morena, em Portugal. Cuadernos do Laboratorio Xeoloxico de Laxe 16, 221-250, 1991.
789
790 Pastor-Galán, D., Ursem, B., Meere, P.A., and Langereis, C.: Extending the Cantabrian Orocline to two
791 continents (from Gondwana to Laurussia). Paleomagnetism from South Ireland. Earth and Planetary
792 Science Letters 432, 223-231, 2015.
793
794 Pereira, M.F., Gama, C., Dias da Silva, Í., Fuenlabrada, J.M., Silva, J.B. and Medina, J.: Isotope
795 geochemistry evidence for Laurussian-type sources of South-Portuguese Zone Carboniferous turbidites
796 (Variscan orogeny). In: Murphy, J.B. (Eds). Pannotia to Pangea: Neoproterozoic and Paleozoic orogenic
797 cycles in the circum-North Atlantic region. Geological Society of London, Special Publication, DOI:
798 10.1144/SP503-2019-163, 2020.
799
800 Pereira, M.F., Martínez Poyatos, D., Pérez-Cáceres, I., Gama, C. and Azor, A.: Comment on
801 ‘‘Stratigraphy of the Northern Pulo do Lobo Domain, SW Iberia Variscides: A palynological
802 contribution’’ by Zélia Pereira et al. (2018) - Geobios 51, 491-506. Geobios 55: 103-106, 2019.
803
804 Pereira, M.F., Gutiérrez-Alonso, G., Murphy, J.B., Drost, K., Gama, C.and Silva, J.B.: Birth and demise
805 of the Rheic Ocean magmatic arc(s): Combined U-Pb and Hf isotope analyses in detrital zircon from SW
806 Iberia siliciclastic strata. Lithos 278-281, 383-399, 2017a.
807
808 Pereira, M.F., Gama, C. and Rodríguez, C.: Coeval interaction between magmas of contrasting
809 composition (Late Carboniferous-Early Permian Santa Eulália-Monforte massif, Ossa-Morena Zone):
810 field relationships and geochronological constraints. Geologica Acta 15, 409-428, 2017b.
811
812 Pereira, M.F., Chichorro, M., Moita, P., Santos, J.F., Solá, A.M.R., Williams, I.S., Silva, J.B. and
813 Armstrong, R.A.: The multistage crystallization of zircon in calc-alkaline granitoids: U-Pb age constraints
814 on the timing of Variscan tectonic activity in SW Iberia. International Journal of Earth Sciences 104, 5,
815 1167-1183, 2015a.
816
817 Pereira, M.F., Castro, A. and Fernández, C.: The inception of a Paleotethyan magmatic arc in Iberia.
818 Geosciences Frontiers: 6, 297-306, 2015b.
819
820 Pereira, M.F., Ribeiro, C., Vilallonga, F., Chichorro, M., Drost, K., Silva, J.B., Albardeiro, L., Hofmann,
821 M. and Linnemann, U.: Variability over time in the sources of South Portuguese Zone turbidites:

evidence of denudation of different crustal blocks during the assembly of Pangea. International Journal of Earth Sciences, 103, 1453-1470, 2014a.

Pereira, M.F., Castro, A., Chichorro, M., Fernández, C., Diaz-Alvarado, J., Martí, J. and Rodriguez, C.: Chronological link between deep-seated processes in magma chambers and eruptions: Permo-Carboniferous magmatism in the core of Pangaea (Southern Pyrenees). Gondwana Research 25, 290-308, 2014b.

Pereira, M.F., Chichorro, M., Johnston, S., Gutiérrez-Alonso, G., Silva, J., Linnemann, U., Hofmann, M. and Drost, K.: The missing Rheic ocean magmatic arcs: provenance analysis of Late Paleozoic sedimentary clastic rocks of SW Iberia. Gondwana Research 22, 882-891, 2012a.

Pereira, M.F., Chichorro, M., Silva, J., Ordóñez-Casado, B., Lee, J. and Williams, I.: Early Carboniferous wrenching, exhumation of high-grade metamorphic rocks and basin instability in SW Iberia; constrains derived from structural geology and U–Pb and 40Ar-39Ar geochronology. Tectonophysics 558-559, 28-44, 2012b.

Pereira, M.F., Solá, A.R., Chichorro, M., Lopes, L., Gerdes, A. and Silva, J.B.:North-Gondwana assembly, break-up and paleogeography: U-Pb isotope evidence from detrital and igneous zircons of Ediacaran and Cambrian rocks of SW Iberia. Gondwana Research 22(3-4): 866-881, 2012c.

Pereira, M.F., Silva, J.B., Drost, K., Chichorro, M. and Apraiz, A.: Relative timing of transcurrent displacements in northern Gondwana: New U-Pb laser ablation MS-ICP-MS zircon and monazite geochronology of gneisses and sheared granites from the Western Iberian Massif (Portugal). Gondwana Research 17 (2-3), 461-481, 2010.

Pereira, M.F., Chichorro, M., Williams, I.S., Silva, J.B., Fernandez, C., Diaz-Azpiroz, M., Apraiz, A. and Castro, A.: Variscan intra-orogenic extensional tectonics in the Ossa-Morena Zone (Évora-Aracena-Lora del Rio metamorphic belt, SW Iberian Massif): SHRIMP zircon U-Th-Pb geochronology. In: Murphy, J.B., Keppie, J.D., Hynes, A.J. (Eds.), Ancient Orogens and Modern AnaloguesGeological Society, London, Special Publications 327, 215-237, 2009.

Pereira, M.F., Chichorro, M., Williams, I.S. and Silva, J.B.: Zircon U-Pb geochronology of paragneisses and biotite granites from the SW Iberia Massif. (Portugal): evidence for a paleogeographic link between the Ossa-Morena Ediacaran basins and the West African craton. In: Ennih, N., Liégeois, J.P. (Eds.), The Boundaries of the West African Craton. Geological Society Special Publication, London 297, 385-408, 2008.

Pereira, M.F., Silva, J.B., Chichorro, M., Moita, P., Santos, J.F., Apraiz, A. and Ribeiro, C.: Crustal growth and deformational processes in the Northern Gondwana margin: constraints from the Évora

Massif (Ossa-Morena Zone, SW Iberia, Portugal). In: Linnemann, U., Nance, R.D., Kraft, P., Zulauf, G. (Eds.), The evolution of the Rheic Ocean: from Avalonian–Cadomian active margin to Alleghenian-Variscan Collision Special Paper of the Geological Society of America 423, 333-358, 2007.

Pereira,M.F., Chichorro,M., Linnemann, U., Eguiluz, L. and Silva, J.B.: Inherited arc signature in Ediacaran and Early Cambrian basins of the Ossa-Morena Zone (Iberian Massif, Portugal): Paleogeographic link with European and North African correlatives. Precambrian Research 144, 297-315, 2006.

Pérez-Cáceres, I., Poyatos, D.M., Simancas, J.F. and Azor, A.:Testing the Avalonian affinity of the South Portuguese Zone and the Neoproterozoic evolution of SW Iberia through detrital zircon populations. Gondwana Research 42, 177-192, 2017.

Pérez-Cáceres, I., Martínez Poyatos, D., Simancas, J.F. and Azor, A.: The elusive nature of the Rheic Ocean suture in SW Iberia, Tectonics, 34, 2429-2450, 2015a.

Pérez-Cáceres, I., Simancas, J.F., Martínez Poyatos, D., Azor, A. and González Lodeiro, F.: Oblique collision and deformation partitioning in the SW Iberian Variscides. Solid Earth Discussions. 7, 3773-3815, 2015b.

Pin, Ch., Fonseca, P.E., Paquette, J.L., Castro, P. and Matte, Ph.: The ca. 350 Ma Beja igneous complex: a record of transcurrent slab break-off in the southern Iberia Variscan Belt? Tectonophysics 461, 356-377, 2008.

Priem, H.N.A., Boelrijk, N.A.I.M., Hebeda, E.H. and Schermerhorn, L.J.G.: Isotopic ages of the Alcáçovas orthogneiss and the Beja porphyries, South Portugal. Comunicações Serviços Geológicos Portugal 72: 3-7, 1986.

Quesada, C. and Oliveira, J.T.: The Geology of Iberia: A Geodynamic Approach. Volume 2: The Variscan Cycle (Simas, F., volume coordinator). Regional Geology Reviews, Springer, p. 1-542, 2019.

Quesada, C., Fonseca, P.E., Munha, J., Oliveira, J.T. and Ribeiro, A.: The Beja–Acebuches Ophiolite (Southern Iberia Variscan fold belt): geological characterization and significance. Boletin Geológico y Minero 105, 3-49, 1994.

Quesada, C., Robardet, M. and Gabaldon, V.: Ossa-Morena Zone. Stratigraphy. Synorogenic phase (Upper Devonian-Carboniferous-Lower Permian). In: Dallmeyer, R.D., Martínez García, E. (Eds.), Pre-Mesozoic Geology of Iberia. Springer-Verlag, Berlin-Heidelberg, 273-279, 1990.

Ribeiro, A., Munhá, J., Dias, R., Mateus, A., Pereira, E., Ribeiro, L., Fonseca, P., Araújo, A., Oliveira, T., Romão, J., Chaminé, H., Coke, C. and Pedro, J.: Geodynamic evolution of the SW Europe Variscides. Tectonics 26, TC6009, https://doi.org/10.1029/2006TC002058, 2007.

Rodrigues, B., Chew, D.M., Jorge, R.C.G.S., Fernandes, P., Veiga-Pires, C. and Oliveira, J.T.: Detrital zircon geochronology of the Carboniferous Baixo Alentejo Flysch Group (South Portugal); constraints on the provenance and geodynamic evolution of the South Portuguese Zone. Journal of the Geological Society of London, http://dx.doi.org/10.1144/jgs2013-084, 2014.

Rosas, F.M., Marques, F.O., Ballevre, M. and Tassinari, C.: Geodynamic evolution of the SW Variscides: orogenic collapse shown by new tectonometamorphic and isotopic data from western Ossa-Morena Zone, SW Iberia. Tectonics 27, TC0080. https://doi.org/10.1029/2008TC002333, 2008.

Santos, J., Mata, J., Gonçalves, F. and Munhá, J.:Contribuição para o conhecimento Geológico-Petrológico da Região de Santa Susana: O Complexo Vulcano-sedimentar da Toca da Moura. Comunicações dos Serviços Geológicos de Portugal 73 (1-2), 29-48, 1987.

Santos, J.F., Andrade, A.S. and Munhá, J.: Magmatismo orogénico Varisco no limite meridional da Zona de Ossa-Morena. Comunicações dos Serviços Geológicos de Portugal, 76, 91-124, 1990.

Sengör, A.M.C., Özeren, S., Zor, E. and Genç, T.: East Anatolian high plateau as a mantle-supported, N-S shortened domal structure: Geophysical Research Letters, v. 30, no. 24, p. 8045, 2003.

Simancas, J.F., Tahiri, A., Azor, A., González Lodeiro, F., Martínez Poyatos, D. and El Hadi, H.: The tectonic frame of the Variscan-Alleghanian orogen in southern Europe and northern Africa. Tectonophysics 398, 181-198, 2005.

Simancas, J.F., Carbonell, R., González Lodeiro, F., Pérez Estaún, A., Juhlin, C., Ayarza, P., Kashubin, A., Azor, A., Martínez Poyatos, D., Sáez, R., Almodóvar, G.R., Pascual, E., Flecha, I. and Martí, D.: Transpressional collision tectonics and mantle plume dynamics: the Variscides of southwestern Iberia. Geological Society of London Memoirs, 32, 345-354, 2006

Simancas, J.F., Azor, A., Martínez Poyatos, D.J., Tahiri, A., El Hadi, H., González-Lodeiro,F., Pérez-Estaún, A. and Carbonell, R.: Tectonic relationships of Southwest Iberia with the allochthons of Northwest Iberia and the Moroccan Variscides. Compte Rendus Geoscience 341, 103-113, 2009.

Spencer, C.J., Kirkland, C.L., and Taylor, R.J.M.: Strategies towards statistically robust interpretations of in situ U-Pb zircon geochronology. Geoscience Frontiers 7, 581-589, 2015.

940 Stampfli, G.M., von Raumer, J. and Borel, G.D.: The Palaeozoic evolution of pre-Variscan terranes: from
941 peri-Gondwana to the Variscan collision. In: Martinez-Catalan, J.R., Hatcher, R.D., Arenas, R., Diaz
942 Garcia, F. (Eds.), Variscan Appalachian Dynamics: The Building of the Upper Paleozoic Basement.
943 Geological Society of America Special Paper, 364, 263-280, 2002.
944
945 Stampfli, G.M., Hochard, C., Vérard, C., Wilhem, C. and von Raumer, J.: The formation of Pangea.
946 Tectonophysics 593, 1-19, 2013.
947
948 Stampfli, G.M. and Kozur, H.W.: Europe from the Variscan to the Alpine Cycles. In: Gee, D.G.,
949 Stephenson, R.A. (Eds.), European Lithosphere Dynamics. Geological Society of London Memoirs 32,
950 57-82, 2006.
951
952 Teixeira, C.: Sobre a flora fossil do Carbónico alentejano. Boletim do Museu do Laboratório de geologia,
953 Universidade de Lisboa, 3ª série, 7-8: 83-100, 1938-1940.
954
955 Teixeira, C.: Sur quelques insectes fossiles du Carbonifere de l'Alentejo. Anais Faculdade de Ciências,
956 Porto, vol. XXVI, 2: 117-120, 1941.
957
958 Teixeira, C.: O Antracolítico continental português. (Estratigrafia- Tectónica). Boletim da Sociedade
959 Geológica, porto, vol. 5, Fasc.1-2: 1-139, 1944.
960
961 Torsvik, T.H., Van der Voo, R., Preeden, U., Mac Niocaill, C., Steinberger, B., Doubrovine, P.V., van
962 Hinsbergen, D.J.J., Domeier, M., Gaina, C., Tohve, E., Meert, J.G., McCausland, P.J.A. and Cocks, R.M.:
963 Phanerozoic polar wander, paleogeography and dynamics. Earth-Science Reviews 114, 325-368, 2012.
964
965 Vermeesch, P.: Multi-sample comparison of detrital age distributions. Chemical Geology 341, 140-146,
966 2013.
967
968 Vermeesch, P.: IsoplotR: A free and open toolbox for geochronology. Geoscience Frontiers 9, 5, 1479-
969 1493, 2018
970
971 von Raumer, J.F., Nesbor, H.-D. and Stampfli, G.M.: The north-subducting Rheic Ocean during the
972 Devonian: consequences for the Rhenohercynian ore sites. International Journal of Earth Sciences
973 (Geologische Rundschau). http://dx.doi.org/10.1007/ s00531-016-1425-x., 2016.
974
975 Wagner, R.H. and Lemos de Sousa, M.J.: The Carboniferous megafloras of Portugal-a revision of
976 identifications and discussion of stratigraphic ages. In: Sousa, M.J.L., Oliveira, J.T. (Eds.), The
977 Carboniferous of Portugal. Memórias dos Serviços Geológicos de Portugal, Lisboa, pp. 127-152, 1983.
978

Wissink G.K., Wilkinson, B.H., and Hoke, G.D: Pairwise sample comparisons and multidimensional scaling of detrital zircon ages with examples from the North American platform, basin, and passive margin settings. Lithosphere 10, 3, 478-491, 2018.

Yamaji, A.: Slab rollback suggested by latest Miocene to Pliocene forearc stress and migration of volcanic front in southern Kyushu, northern Ryukyu Arc. Tectonophysics 364, 9-24, 2003.

Figure captions

Figure 1: A- Inset with location of SW Iberia in the Iberian Variscan belt with regional distribution of the main Paleozoic terranes: CIZ- Central Iberian Zone; CZ- Cantabrian Zone; GTMZ- Galicia-Trás-os-Montes Zone; OMZ- Ossa-Morena Zone; PLZ- Pulo do Lobo Zone; SPZ- South-Portuguese Zone and WALZ- West Asturian-Leonese Zone. B- Simplified Geological Map of SW Iberia showing the South-Portuguese, Pulo do Lobo and Ossa-Morena zones (Modified from Pereira et al. 2017a, 2019 and references therein; Quesada and Oliveira, 2019).

Figure 2: Simplified geological map and schematic stratigraphy of the Santa Susana-São Cristovão region (Ossa-Morena Zone; Modified from Gonçalves and Carvalhosa, 1984; Machado et al., 2012). Sampling locations of the Carboniferous sedimentary and igneous rocks used for geochronology are indicated with yellow stars.

Figure 3: Photographs of the Carboniferous igneous rocks of the Santa Susana-São Cristovão region: A- Baleizão porphyry intrusive contact (yellow arrow) with siliciclastic rocks of the Toca da Moura volcano-sedimentary complex; B- Baleizão porphyry; C-D- Rhyolitic tuffs of the Toca da Moura volcano-sedimentary complex; E- Volcanic breccia with fragments of siltstone (black) and rhyolite (yellow) at the base of the silicic tuffs from the Toca da Moura volcano-sedimentary complex; F- Silicic volcanic rock interbedded with siltstones of the Cabrela volcano-sedimentary complex.

Figure 4: Photographs of the Carboniferous sedimentary rocks of the Santa Susana Formation lower member: A- View of dipping meter-thick beds of medium-coarse grained sandstone intercalated with conglomerate; B- Planar-bedded coarse-grained sandstone; C- Plant imprints in sandstone; D- Conglomerate with cobbles and pebbles of granite (G), quartzite (Q), silicic porphyry (SP) and mafic volcanic rock (M); E- Conglomerate with pebbles of rhyolite (R), phyllite (P), felsic tuff (T) and quartzite (Q).

Figure 5: Petrographic images of the Carboniferous sedimentary and igneous rocks of the Santa Susana-São Cristovão region: A- Rhyolitic-rhyodacitic tuff of the Toca da Moura volcano-sedimentary complex showing quartz and feldspar phenocrysts enclosed in ash matrix; B- Rhyolitic tuff showing flattened dark-brown millimeter-sized pumice and lithoclasts enclosed in ash matrix; C- Porphyritic texture of the Baleizão rhyodacite-rhyolite characterized by quartz, plagioclase, K-feldspar, biotite and amphibole phenocryst embedded in a fine-grained silicic matrix; D- Cobble of fine-grained granite showing graphic intergrowths of quartz and alkali feldspar, found in conglomerate from the Santa Susana Formation; E- Siltstone of the Toca da Moura volcano-sedimentary complex mostly composed of quartz grains and a few grains of plagioclase (P), tourmaline (T), and rock fragments (L); F- Siltstone of the Cabrela volcano-sedimentary complex showing fining upwards grading and a slump-fold; G-H, Sandstones from the Santa Susana Formation with high percentage of lithoclasts (L) and a few feldspar (F).

Figure 6: Concordia diagrams, weighted mean of $^{206}Pb/^{238}U$ ages of analyzed zircon grains extracted from silicic volcanic rocks of the Toca da Moura and Cabrela volcano-sedimentary complex.

Figure 7: Concordia diagrams, weighted mean of $^{206}Pb/^{238}U$ ages of analyzed zircon grains of: A- the Baleizão porphyry and B- the cobble of granite found in conglomerate from the Santa Susana Formation.

Figure 8: Pie diagrams and Kernel Density Estimation (KDE) with U-Pb detrital-zircon ages of siliciclastic rocks from: A- the Toca da Moura (TM-3, this study) and Cabrela (CB: CBR-11, this study; and OM-200, Pereira et al., 2012a) volcano-sedimentary complexes, and B- the Santa Susana Formation (SS-1 and SS-2, this study; and SS Upper member, StSz2 and StSz4 from Dinis et al., 2018); C- U-Pb age cumulative frequency plots applied to the U-Pb ages (90-110% concordance) of detrital zircon grains from the Toca da Moura and Cabrela volcano-sedimentary complexes, and the Santa Susana Formation.

Figure 9: Multi-Dimensional Scaling diagrams (Vermeesch, 2018) applied to the U-Pb ages (90-110% concordance) of detrital zircon grains from the Toca da Moura (TM-3) and Cabrela (CB) volcano-sedimentary complexes, and the Santa Susana Formation (SS1, SS2, SS upper member), and different potential sources: OMZ (Linnemann et al. 2008; Pereira et al. 2008, 2012c), PLZ (Pereira et al. 2017a; Pérez Cácerez et al. 2017), SPZ (Braid et al. 2011; Pereira et al., 2012a, 2014a; Rodrigues et al. 2014). Abbreviations: MT- Mértola Formation; MR- Mira formation; BJ- Brejeira formation; PQ-TRC- Phyllite-Quartzite and Tercenas formations; SI-

REP- Santa Iria and Represa formations; P-G-R-A-R- Pulo do Lobo, Gafo, Ribeira de Lima, Atalaia and Ronquillo formations; HT- Horta da Torre Formation.

Figure 10: Sketches showing inferred tectonic evolution and sedimentation recorded in SW Iberia Carboniferous stratigraphy during Laurussian-Gondwana oblique collision (Modified from Pereira et al., 2012b; 2020); A- Late Devonian; B1-B2- Early Carboniferous; C1-C2- Late Carboniferous.

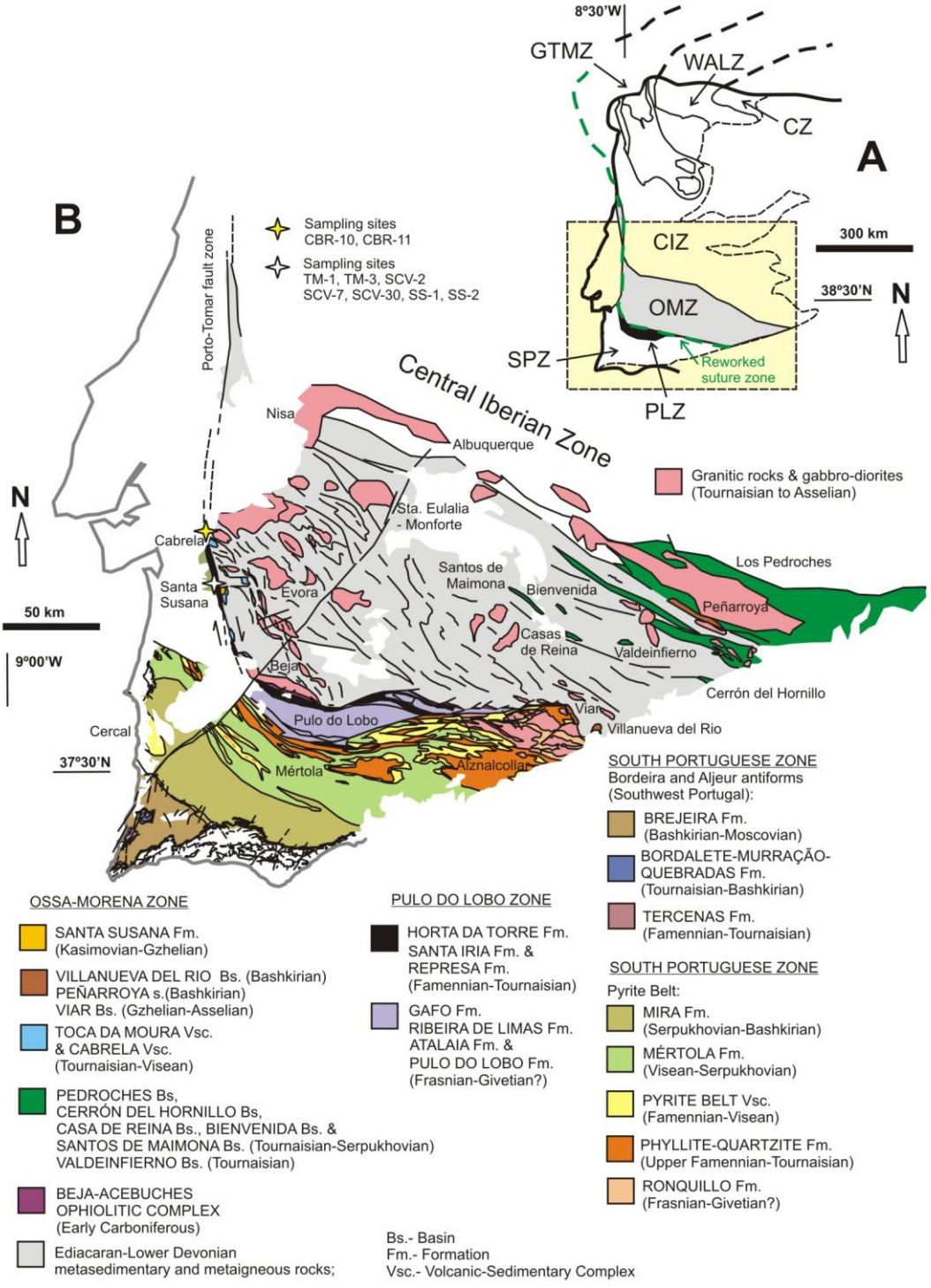
8°30'W
GTMZ
WALZ
CZ
A
CIZ
OMZ
SPZ
PLZ
Reworked suture zone
300 km
38°30'N
N
B
Sampling sites
CBR-10, CBR-11
Sampling sites
TM-1, TM-3, SCV-2
SCV-7, SCV-30, SS-1, SS-2
Porto-Tomar fault zone
Central Iberian Zone
Granitic rocks & gabbro-diorites
(Tournaisian to Asselian)
Nisa
Albuquerque
Sta. Eulalia
- Monforte
Cabrela
Santa
Susana
Evora
Santos de
Maimona
Bienvenida
Los Pedroches
Peñarroya
Casas
de Reina
Valdeinfierno
Cerrón del Hornillo
Viar
Villanueva del Rio
Beja
Pulo do Lobo
Cercal
37°30'N
Mértola
Alznalcollar
50 km
9°00'W
SOUTH PORTUGUESE ZONE
Bordeira and Aljeur antiforms
(Southwest Portugal):
BREJEIRA Fm.
(Bashkirian-Moscovian)
BORDALETE-MURRAÇÃO-
QUEBRADAS Fm.
(Tournaisian-Bashkirian)
TERCENAS Fm.
(Famennian-Tournaisian)
SOUTH PORTUGUESE ZONE
Pyrite Belt:
MIRA Fm.
(Serpukhovian-Bashkirian)
MÉRTOLA Fm.
(Visean-Serpukhovian)
PYRITE BELT Vsc.
(Famennian-Visean)
PHYLLITE-QUARTZITE Fm.
(Upper Famennian-Tournaisian)
RONQUILLO Fm.
(Frasnian-Givetian?)
OSSA-MORENA ZONE
SANTA SUSANA Fm.
(Kasimovian-Gzhelian)
VILLANUEVA DEL RIO Bs. (Bashkirian)
PEÑARROYA s.(Bashkirian)
VIAR Bs. (Gzhelian-Asselian)
TOCA DA MOURA Vsc.
& CABRELA Vsc.
(Tournaisian-Visean)
PEDROCHES Bs,
CERRÓN DEL HORNILLO Bs,
CASA DE REINA Bs., BIENVENIDA Bs. &
SANTOS DE MAIMONA Bs. (Tournaisian-Serpukhovian)
VALDEINFIERNO Bs. (Tournaisian)
BEJA-ACEBUCHES
OPHIOLITIC COMPLEX
(Early Carboniferous)
Ediacaran-Lower Devonian
metasedimentary and metaigneous rocks;
PULO DO LOBO ZONE
HORTA DA TORRE Fm.
SANTA IRIA Fm. &
REPRESA Fm.
(Famennian-Tournaisian)
GAFO Fm.
RIBEIRA DE LIMAS Fm.
ATALAIA Fm. &
PULO DO LOBO Fm.
(Frasnian-Givetian?)
Bs.- Basin
Fm.- Formation
Vsc.- Volcanic-Sedimentary Complex

Figure 1

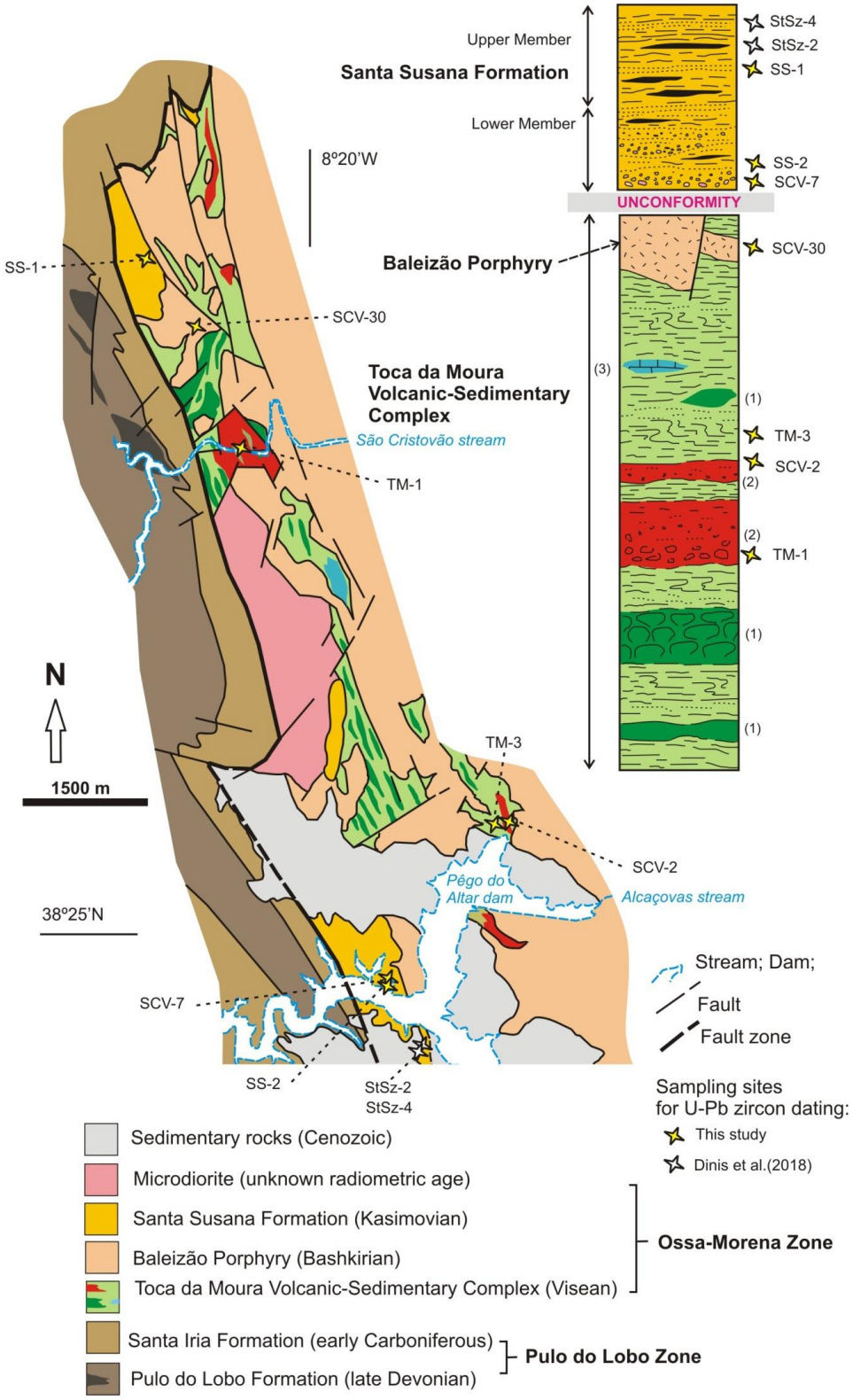
Upper Member
Santa Susana Formation
Lower Member
StSz-4
StSz-2
SS-1
SS-2
SCV-7
UNCONFORMITY
Baleizão Porphyry
SCV-30
Toca da Moura
Volcanic-Sedimentary
Complex
São Cristovão stream
TM-1
TM-3
SCV-2
(3)
(1)
(2)
8°20'W
SS-1
SCV-30
N
1500 m
38°25'N
TM-3
SCV-2
Pégo do
Altar dam
Alcaçovas stream
SCV-7
SS-2
StSz-2
StSz-4
Stream; Dam;
Fault
Fault zone
Sampling sites
for U-Pb zircon dating:
This study
Dinis et al.(2018)
Sedimentary rocks (Cenozoic)
Microdiorite (unknown radiometric age)
Santa Susana Formation (Kasimovian)
Baleizão Porphyry (Bashkirian)
Toca da Moura Volcanic-Sedimentary Complex (Visean)
Ossa-Morena Zone
Santa Iria Formation (early Carboniferous)
Pulo do Lobo Formation (late Devonian)
Pulo do Lobo Zone

Figure 2

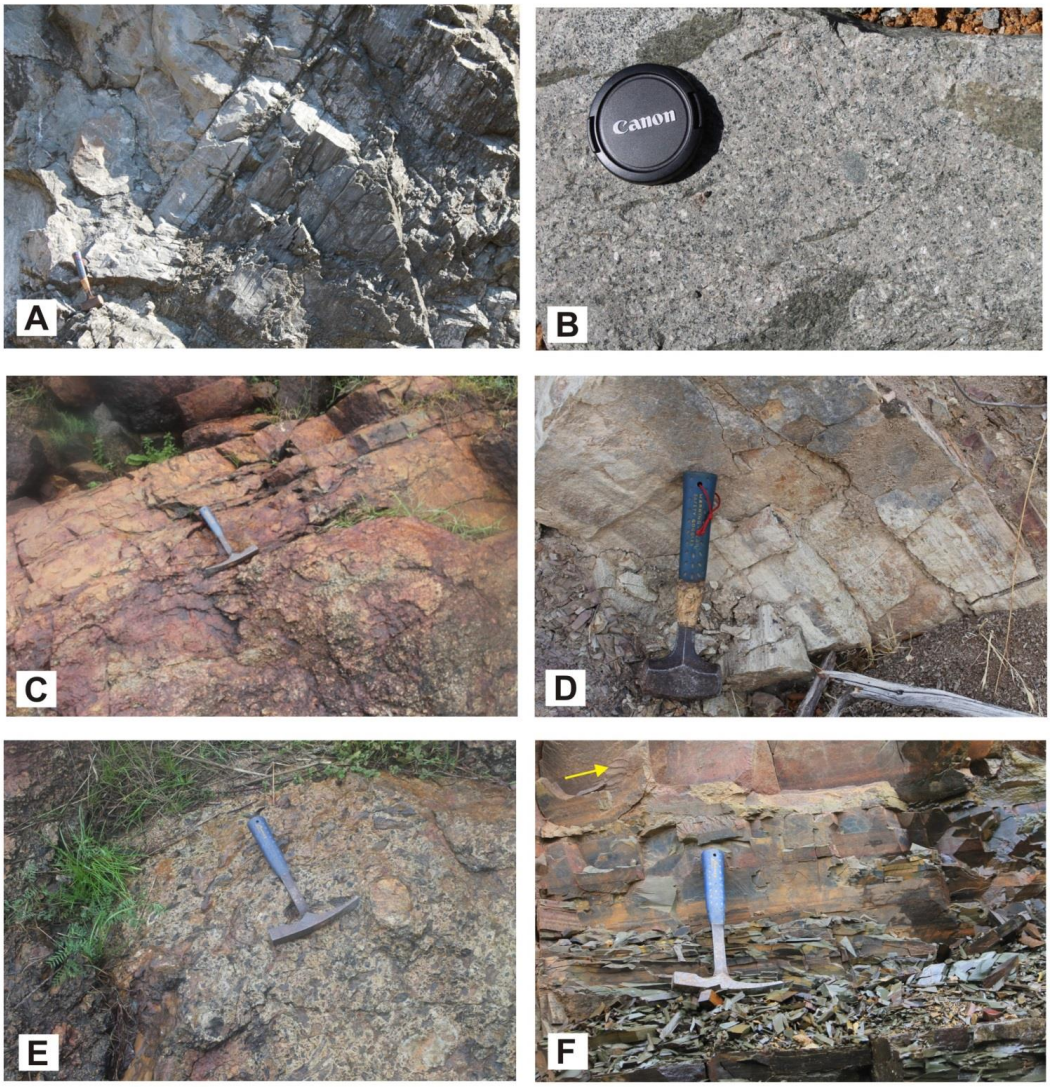

Figure 3

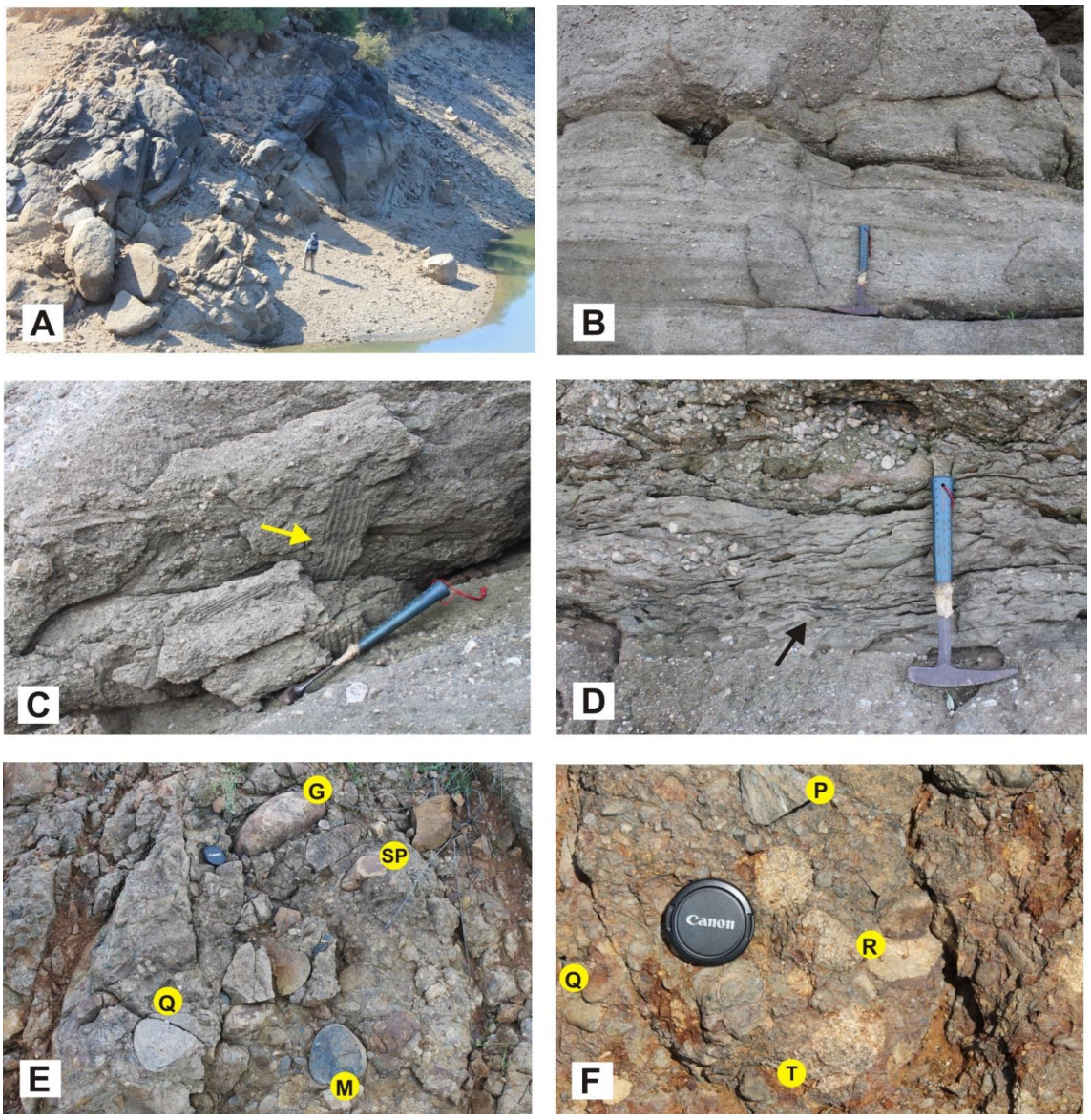

Figure 4

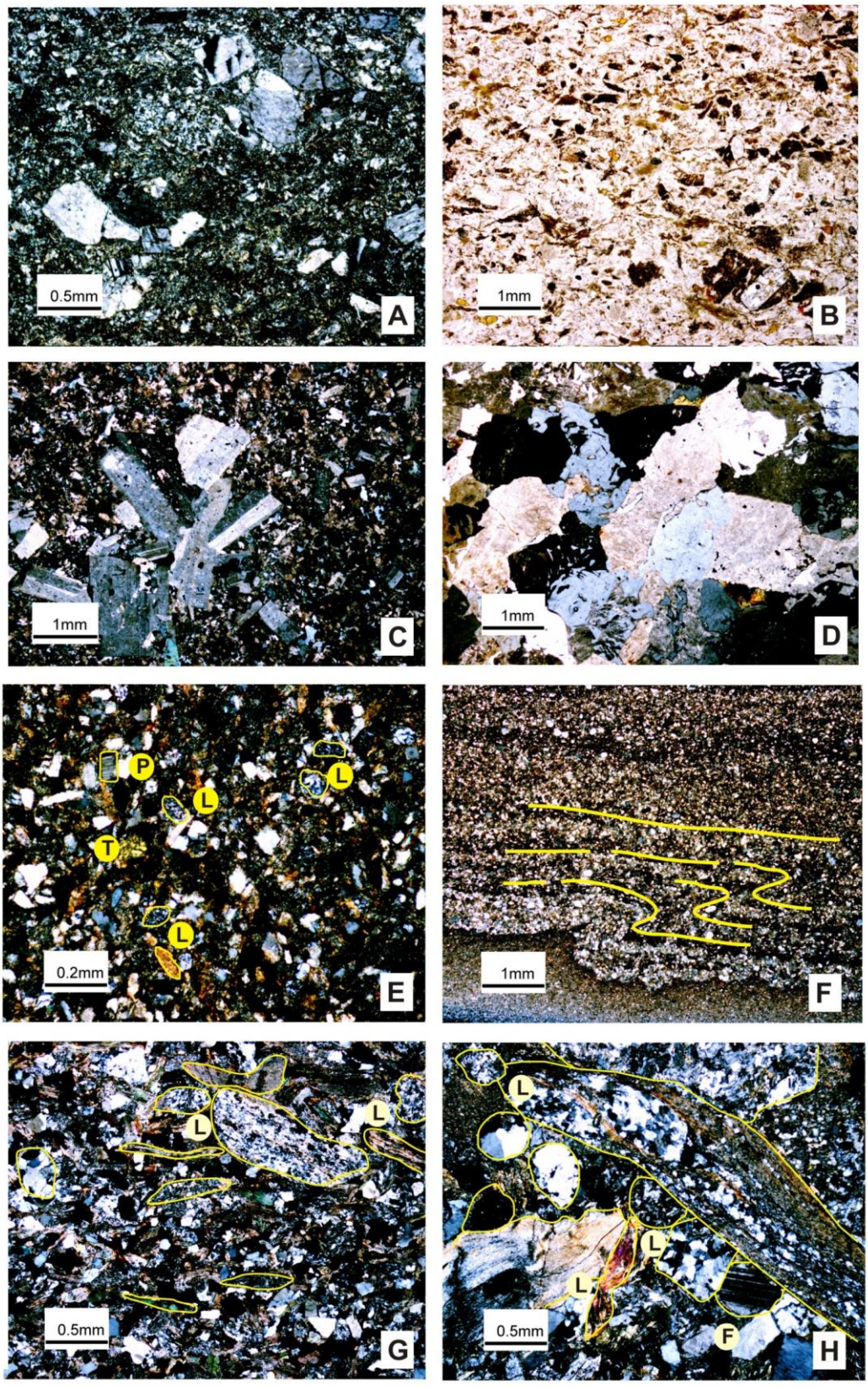

Figure 5

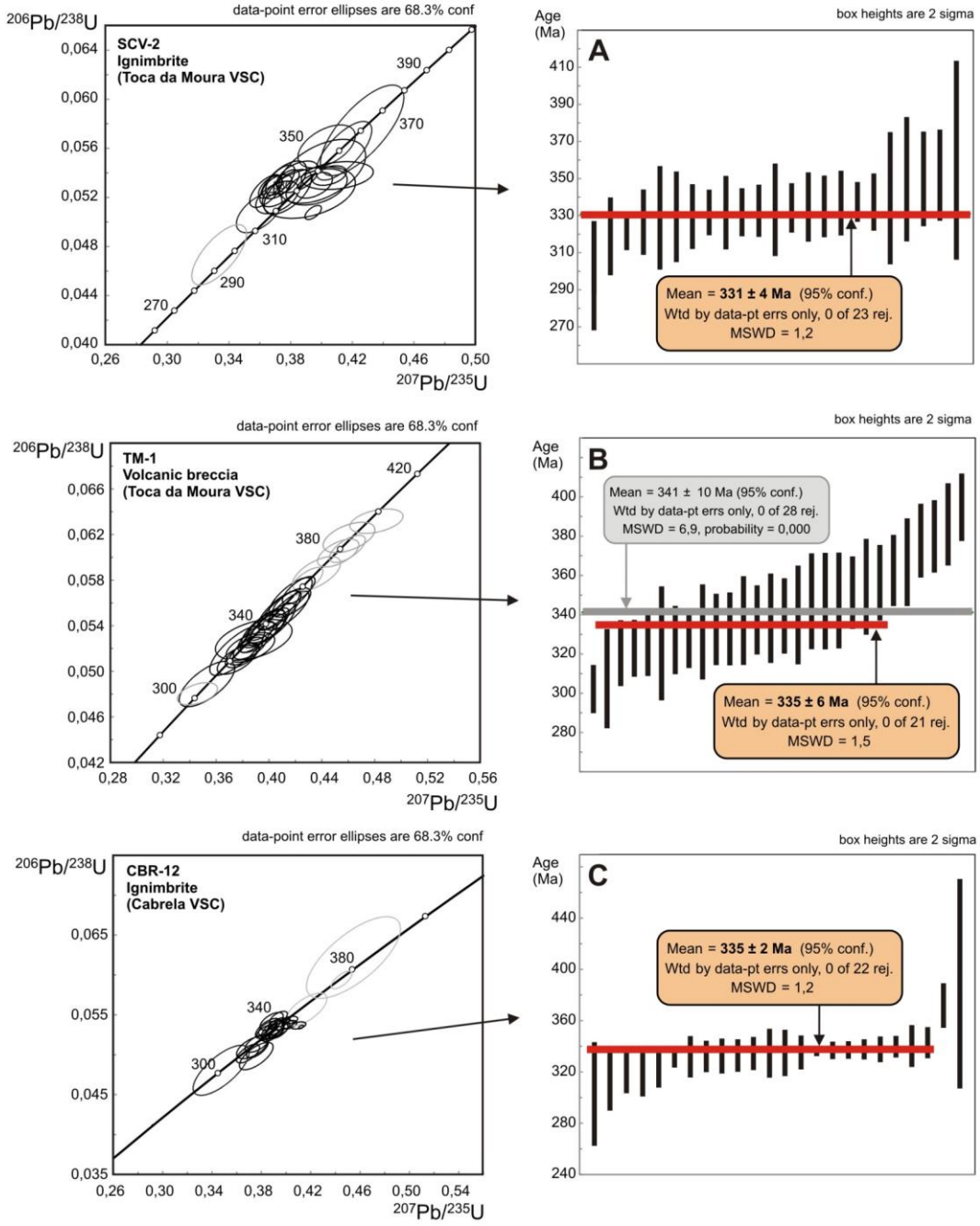
data-point error ellipses are 68.3% conf
206Pb/238U
SCV-2
Ignimbrite
(Toca da Moura VSC)
207Pb/235U
box heights are 2 sigma
Age (Ma)
A
Mean = 331 ± 4 Ma (95% conf.)
Wtd by data-pt errs only, 0 of 23 rej.
MSWD = 1,2
TM-1
Volcanic breccia
(Toca da Moura VSC)
B
Mean = 341 ± 10 Ma (95% conf.)
Wtd by data-pt errs only, 0 of 28 rej.
MSWD = 6,9, probability = 0,000
Mean = 335 ± 6 Ma (95% conf.)
Wtd by data-pt errs only, 0 of 21 rej.
MSWD = 1,5
CBR-12
Ignimbrite
(Cabrela VSC)
C
Mean = 335 ± 2 Ma (95% conf.)
Wtd by data-pt errs only, 0 of 22 rej.
MSWD = 1,2

Figure 6

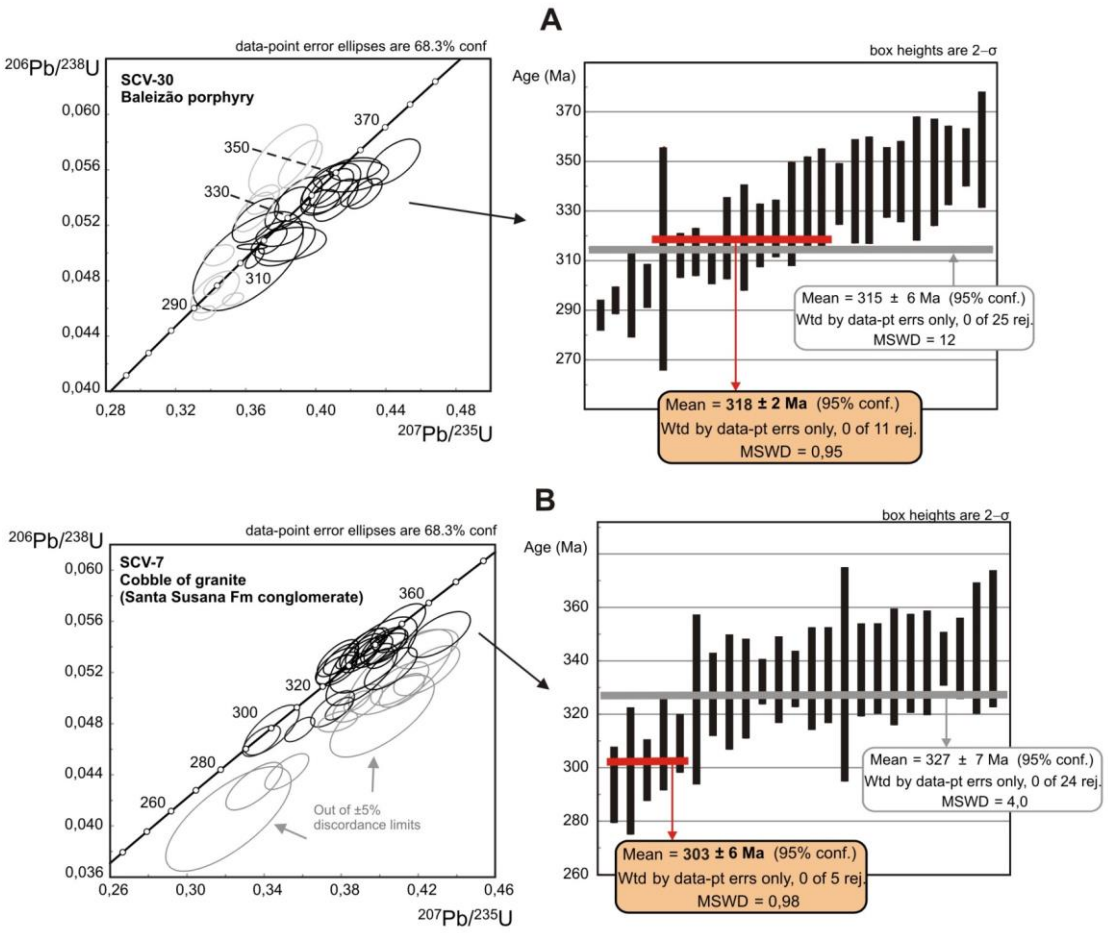
A
data-point error ellipses are 68.3% conf
box heights are 2–σ
SCV-30
Baleizão porphyry
206Pb/238U
207Pb/235U
Age (Ma)
Mean = 315 ± 6 Ma (95% conf.)
Wtd by data-pt errs only, 0 of 25 rej.
MSWD = 12
Mean = 318 ± 2 Ma (95% conf.)
Wtd by data-pt errs only, 0 of 11 rej.
MSWD = 0,95
B
data-point error ellipses are 68.3% conf
box heights are 2–σ
SCV-7
Cobble of granite
(Santa Susana Fm conglomerate)
Out of ±5% discordance limits
Mean = 327 ± 7 Ma (95% conf.)
Wtd by data-pt errs only, 0 of 24 rej.
MSWD = 4,0
Mean = 303 ± 6 Ma (95% conf.)
Wtd by data-pt errs only, 0 of 5 rej.
MSWD = 0,98

Figure 7

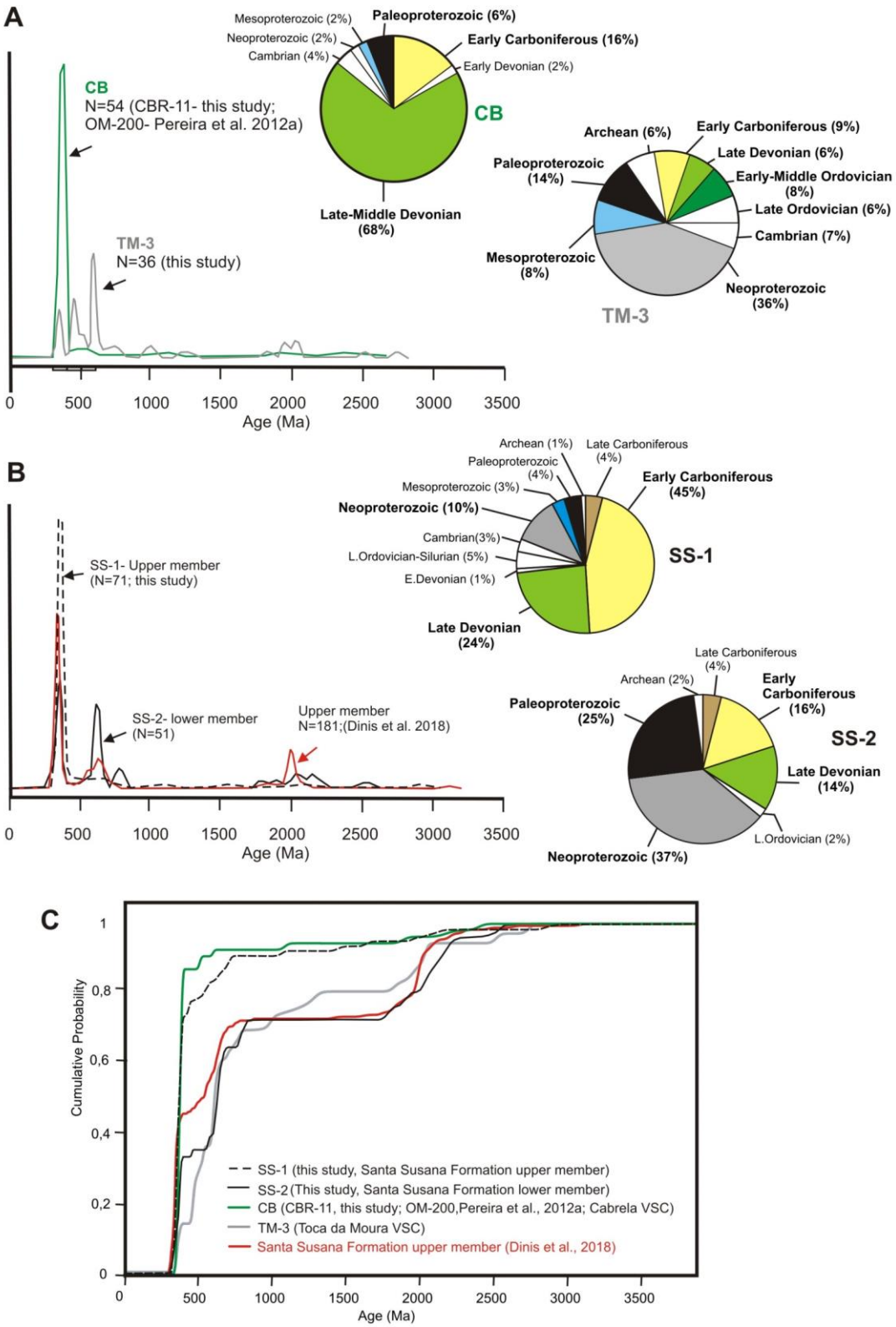
A
CB
N=54 (CBR-11- this study;
OM-200- Pereira et al. 2012a)
TM-3
N=36 (this study)
Age (Ma)
Mesoproterozoic (2%)
Paleoproterozoic (6%)
Neoproterozoic (2%)
Early Carboniferous (16%)
Cambrian (4%)
Early Devonian (2%)
Late-Middle Devonian
(68%)
Archean (6%)
Early Carboniferous (9%)
Late Devonian (6%)
Paleoproterozoic
(14%)
Early-Middle Ordovician
(8%)
Late Ordovician (6%)
Cambrian (7%)
Mesoproterozoic
(8%)
Neoproterozoic
(36%)
B
SS-1- Upper member
(N=71; this study)
SS-2- lower member
(N=51)
Upper member
N=181;(Dinis et al. 2018)
Archean (1%)
Late Carboniferous
(4%)
Paleoproterozoic
(4%)
Early Carboniferous
(45%)
Mesoproterozoic (3%)
Neoproterozoic (10%)
Cambrian(3%)
L.Ordovician-Silurian (5%)
E.Devonian (1%)
Late Devonian
(24%)
Late Carboniferous
(4%)
Archean (2%)
Early
Carboniferous
(16%)
Paleoproterozoic
(25%)
Late Devonian
(14%)
L.Ordovician (2%)
Neoproterozoic (37%)
C
Cumulative Probability
SS-1 (this study, Santa Susana Formation upper member)
SS-2 (This study, Santa Susana Formation lower member)
CB (CBR-11, this study; OM-200,Pereira et al., 2012a; Cabrela VSC)
TM-3 (Toca da Moura VSC)
Santa Susana Formation upper member (Dinis et al., 2018)
Age (Ma)

Figure 8

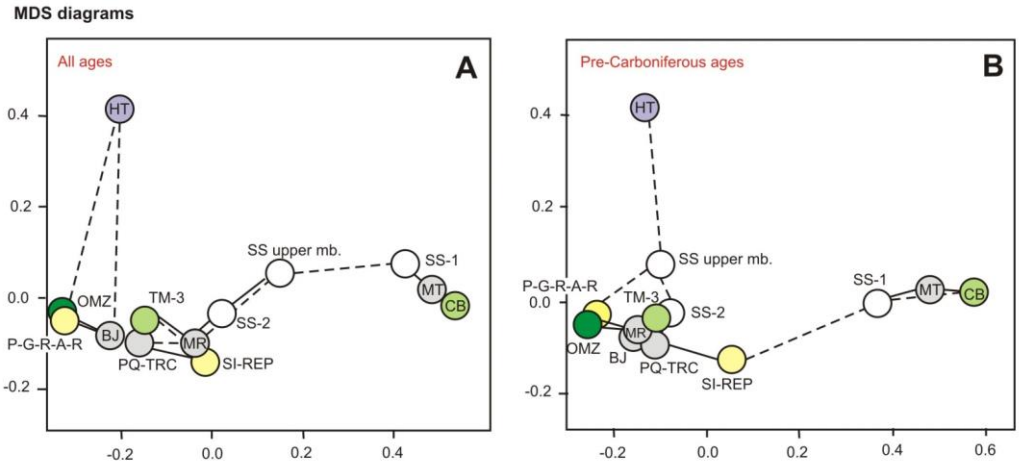
MDS diagrams
All ages
A
HT
SS upper mb.
SS-1
MT
CB
OMZ
TM-3
SS-2
BJ
MR
P-G-R-A-R
PQ-TRC
SI-REP
0.4
0.2
0.0
-0.2
-0.2
0.0
0.2
0.4
Pre-Carboniferous ages
B
HT
SS upper mb.
SS-1
MT
CB
P-G-R-A-R
TM-3
SS-2
MR
OMZ
BJ
PQ-TRC
SI-REP
0.4
0.2
0.0
-0.2
-0.2
0.0
0.2
0.4
0.6

Figure 9

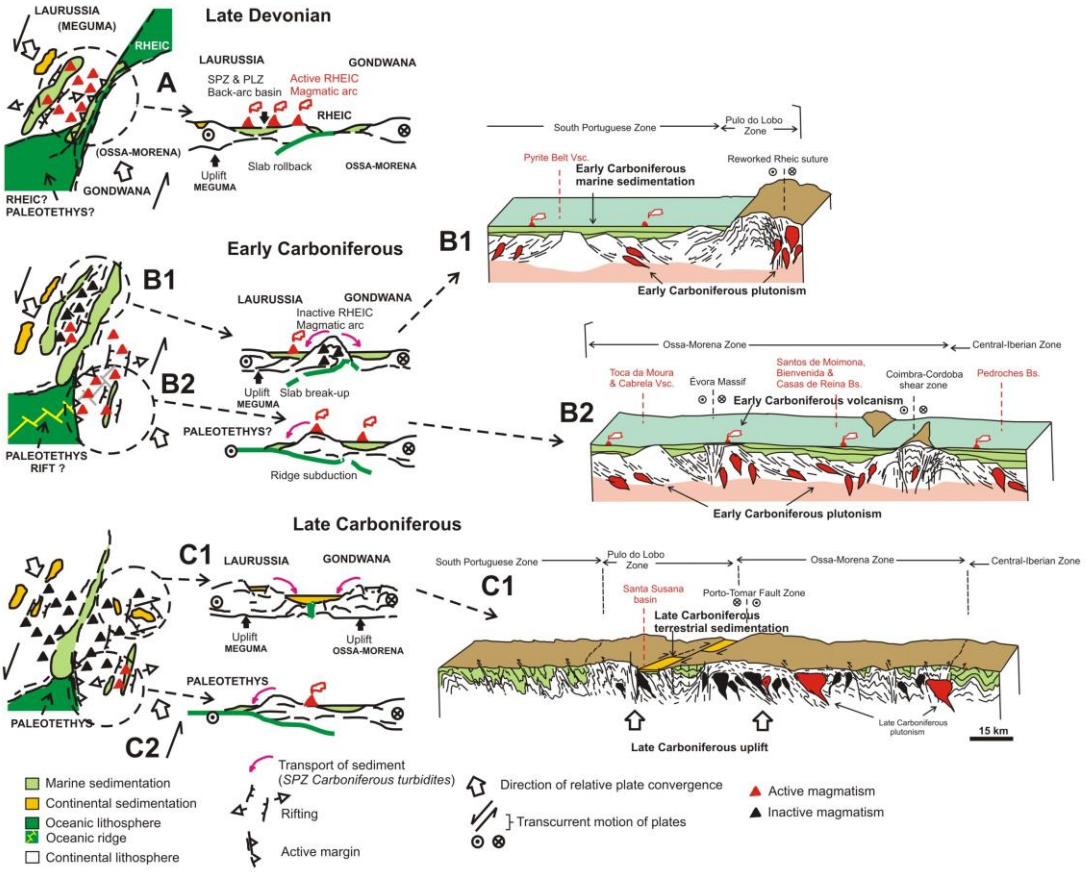
Late Devonian
LAURUSSIA
(MEGUMA)
RHEIC
A
(OSSA-MORENA)
GONDWANA
RHEIC?
PALEOTETHYS?
LAURUSSIA
GONDWANA
SPZ & PLZ
Back-arc basin
Active RHEIC
Magmatic arc
RHEIC
Uplift
MEGUMA
Slab rollback
OSSA-MORENA
Early Carboniferous
B1
B2
LAURUSSIA
GONDWANA
Inactive RHEIC
Magmatic arc
Uplift
MEGUMA
Slab break-up
PALEOTETHYS?
Ridge subduction
PALEOTETHYS
RIFT ?
South Portuguese Zone
Pulo do Lobo
Zone
Pyrite Belt Vsc.
Early Carboniferous
marine sedimentation
Reworked Rheic suture
Early Carboniferous plutonism
Ossa-Morena Zone
Central-Iberian Zone
Toca da Moura
& Cabrela Vsc.
Évora Massif
Santos de Moimona,
Bienvenida &
Casas de Reina Bs.
Coimbra-Cordoba
shear zone
Pedroches Bs.
Early Carboniferous volcanism
Early Carboniferous plutonism
Late Carboniferous
C1
C2
LAURUSSIA
GONDWANA
Uplift
MEGUMA
Uplift
OSSA-MORENA
PALEOTETHYS
PALEOTETHYS
South Portuguese Zone
Pulo do Lobo
Zone
Ossa-Morena Zone
Central-Iberian Zone
Santa Susana
basin
Porto-Tomar Fault Zone
Late Carboniferous
terrestrial sedimentation
Late Carboniferous plutonism
15 km
Late Carboniferous uplift
Marine sedimentation
Continental sedimentation
Oceanic lithosphere
Oceanic ridge
Continental lithosphere
Transport of sediment
(SPZ Carboniferous turbidites)
Rifting
Active margin
Direction of relative plate convergence
Transcurrent motion of plates
Active magmatism
Inactive magmatism

Figure 10